arXiv:hep-ph/9912260v2 18 Jan 2000

KEK-TH-648
SNS-PH/99-16
hep-ph/9912260

Supersymmetry versus precision experiments revisited

Gi-Chol Cho[*,1),2)] **and Kaoru Hagiwara**[1)]

1) *Theory Group, KEK, Tsukuba, Ibaraki 305-0801, Japan*
2) *Scuola Normale Superiore, Piazza dei Cavalieri 7, I-56126 Pisa, Italy*

Abstract

We study constraints on the supersymmetric standard model from the updated electroweak precision measurements — the Z-pole experiments and the W-boson mass measurements. The supersymmetric-particle contributions to the universal gauge-boson-propagator corrections are parametrized by the three oblique parameters S_Z, T_Z and m_W. The oblique corrections, the Zqq and Zll vertex corrections, and the vertex and box corrections to the μ-decay width are separately studied in detail. We first study individual contribution from the four sectors of the model, the squarks, the sleptons, the supersymmetric fermions (charginos and neutralinos), and the supersymmetric Higgs bosons, to the universal oblique parameters, where the sum of individual contributions gives the total correction. We find that the light squarks or sleptons, whose masses just above the present direct search limits, always make the fit worse than that of the Standard Model (SM), whereas the light charginos and neutralinos generally make the fit slightly better. The contribution from the supersymmetric Higgs sector is found small. We then study the vertex/box corrections carefully when both the supersymmetric fermions (-inos) and the supersymmetric scalars (squarks and sleptons) are light, and find that no significant improvement over the SM fit is achieved. The best overall fit to the precision measurements are found when charginos of mass ~ 100 GeV with a dominant wino-component are present and the doublet squarks and sleptons are all much heavier. The improvement over the SM is marginal, however, where the total χ^2 of the fit to the 22 data points decreases by about one unit, due mainly to a slightly better fit to the Z-boson total width.

PACS: 11.30.Pb, 12.15.Lk, 12.60.Jv
Keywords: Supersymmetry, electroweak precision measurement, radiative correction

---

[*] Research Fellow of the Japan Society for the Promotion of Science

1 Introduction

The supersymmetric standard model has been the leading candidate for the theory beyond the Standard Model (SM) of elementary particles. The supersymmetry (SUSY), the symmetry between bosons and fermions, gives us an elegant solution [1] to the hierarchy problem [2, 3], the stability of the electroweak scale (~ 100 GeV) against the more fundamental scale of physics, the Grand Unified Theory (GUT) scale ($\sim 10^{16}$ GeV) where the three gauge interactions may be unified, or the Planck scale ($\sim 10^{19}$ GeV) where the gauge interactions may be unified with the gravity interactions. It also offers us an attractive scenario that the electroweak symmetry breaking may occur radiatively [4] if the top quark is sufficiently heavy but not too much ($100 \text{ GeV} \lesssim m_t \lesssim 200$ GeV) [5]. The observation that the minimal supersymmetric standard model (MSSM) leads to the unification of the three gauge couplings at the 'right' scale, $\sim 2 \times 10^{16}$ GeV, high enough for the proton longevity, if the supersymmetric particles exist with masses at or below the 1 TeV scale [6], and the discovery of the top quark [7] in the 'right' mass range, jointly have made us take the MSSM as a serious candidate for the theory just beyond the present new-particle search front.

Despite the high expectations, however, various efforts in search of an evidence for supersymmetric particles have so far been fruitless. There had been occasions when a short-lived experimental 'anomaly' such as the mismatch of α_s determined from the low-energy experiments and that obtained from the Z-boson decays and/or the significantly large partial width $\Gamma(Z \to b\bar{b})$ as compared to the SM prediction, were considered as a possible evidence for relatively light supersymmetric particles [8, 9, 10]. All such anomalies were short-lived and the precision electroweak data [11] from the completed experiments at LEP1 and the Tevatron run-I, and the on-going experiments at SLC and LEP2 are all consistent with the SM predictions. Alongside, the direct search limits for the supersymmetric particle masses have steadily risen with time. The only additional encouragement from the precision electroweak experiments is that the preferred range of the SM Higgs boson mass is consistent with the stringent upper bound [12, 13, 14, 15, 16] of the lightest Higgs boson mass in the supersymmetric theories. The good news is that the supersymmetric theories have not been ruled out yet, while the bad news is that studies of precision electroweak experiments give us only the lower bounds for the supersymmetric particle masses.

There have recently been numerous attempts [17, 18] to identify constraints on the MSSM parameters from precision electroweak measurements. In this report, we present the first results of our comprehensive study of the constraints on the MSSM parameters from the electroweak precision measurements.

We perform a systematic study of the MSSM parameter space by observing that the concept of the universal gauge-boson-propagator corrections, or the oblique corrections [19, 20, 21, 22], is useful in the MSSM in the sense that they dominate the radiative corrections if either the supersymmetric scalars (squarks and sleptons) or the supersymmetric fermions (charginos and neutralinos) are all sufficiently heavy. In this limit, all the precision measurements on the Z-boson properties can be parametrized by just two oblique parameters, S_Z and T_Z, whereas the W-boson mass itself makes the third oblique parameter. Here we closely follow the formalism developed in refs. [23, 24, 25], slightly modified to suit our MSSM studies. In this limit of the dominant oblique corrections, we can study in detail the contributions of the four sectors of the MSSM separately [26]; the squarks, the sleptons, the supersymmetric fermions (charginos and neutralinos), and the supersymmetric Higgs sector. We find that although the contributions from relatively light squarks and/or sleptons generally make the fit to the electroweak data worse than the SM fit, those from relatively light charginos and neutralinos can slightly improve the fit.

In the second stage, we examine the case where both the supersymmetric scalars and fermions are light, by studying their contributions to the muon lifetime, $\Delta\bar{\delta}_G$, and to all the Z-boson decay amplitudes, Δg_L^ν, Δg_L^e, Δg_R^e, Δg_L^u, Δg_R^u, Δg_L^d, Δg_R^d, $\Delta g_L^{\nu_\tau}$, Δg_L^τ, Δg_R^τ, Δg_L^b, and Δg_R^b. Here Δg_α^f stands for the deviation of the non-oblique correction to the $Zf_\alpha f_\alpha$ vertex from the reference SM prediction. Within our approximation of the MSSM Lagrangian, the amplitudes for the first two generation quarks and leptons are identical, and only the above 12 distinctive corrections appear. Because we find an indication that the existence of relatively light (~ 100 GeV) charginos and neutralinos can somewhat improve the SM fit to the electroweak data, we study the consequences of having light sleptons and/or squarks in addition to the light charginos and neutralinos. We generally find that the goodness of the fit worsens in such cases. Studies of the consequences of more specific models of the supersymmetry breaking mechanism, such as the supergravity models and the gauge-mediated supersymmetry breaking models, will be presented elsewhere [27].

The paper is organized as follows. In section 2, we present the formalism which we calculate all the electroweak observables in the MSSM. The dependences of those observables in terms of the SM parameters, m_t, $m_{H_{\rm SM}}$, $\alpha_s = \alpha_s(m_Z)_{\overline{\rm MS}}$, and $\alpha(m_Z^2)$ are given in a compactly parametrized form [24, 25]. The MSSM Lagrangian and constraints on its parameters are summarized in section 3, and all the MSSM contributions to the one-loop functions are presented in the appendices. In section 4, we study oblique corrections from the squarks and sleptons (sec. 4.1), the supersymmetric Higgs bosons (sec. 4.2), and the supersymmetric fermions (charginos and neutralinos) (sec. 4.3), separately. In section 5, we study consequences of vertex and box corrections in addition to the gauge-boson-propagator corrections: the vertex corrections due to the MSSM Higgs bosons (sec. 5.1), those from squarks and gluinos (sec. 5.2), those from squarks and charginos/neutralinos (sec. 5.3), and the vertex/box corrections from sleptons and charginos/neutralinos (sec. 5.4). In section 6, we examine quantitative significance of the MSSM contributions to the electroweak radiative corrections. Section 7 gives conclusions. Appendix A summarizes our notation [28] for the MSSM mixing matrices and the couplings among the mass eigenstates. Appendix B gives the MSSM contribution to the gauge-boson-propagator corrections and the oblique parameters S, T, U and R. Appendix C gives the MSSM contribution to the Z-boson decay amplitudes. Appendix D gives the MSSM contribution to the muon-decay amplitude.

2 Electroweak observables in the MSSM

In this section, we give all the theoretical predictions for the electroweak observables which are used in our analysis. The experimental data of the Z-pole experiments and the W-boson mass measurement are summarized in Table 1. Because the MSSM predicts slightly different Z-decay amplitudes into the τ-leptons as compared to those into e or μ, we will use in the following analysis the data set which do not assume the e-μ-τ universality. By removing the two entries, R_ℓ and $A_{\rm FB}^{0,\ell}$ that assume the lepton universality, there are 19 data points in the Table. The total χ^2 is obtained by using the correlation matrices of ref. [11].

The reference SM predictions are given in the table for an arbitrarily chosen set of the four inputs, $m_t = 175$ GeV, $m_{H_{\rm SM}} = 100$ GeV, $1/\alpha(m_Z^2) = 128.90$* and $\alpha_s = \alpha_s(m_Z)_{\overline{\rm MS}} = 0.118$. In the following, we present simple parametrizations of the SM predictions for the parameter sets around the above reference point in terms of the normalized variables;

$$x_t = \frac{m_t(\text{GeV}) - 175}{10}, \tag{2.1a}$$

$$x_h = \ln\frac{m_{H_{\rm SM}}(\text{GeV})}{100}, \tag{2.1b}$$

$$x_\alpha = \frac{1/\alpha(m_Z^2) - 128.90}{0.09}, \tag{2.1c}$$

$$x_s = \frac{\alpha_s(m_Z)_{\overline{\rm MS}} - 0.118}{0.003}. \tag{2.1d}$$

The SM predictions for an arbitrary set of the four input parameters (m_t, $m_{H_{\rm SM}}$, $\alpha(m_Z^2)$, $\alpha_s(m_Z)$) are then obtained easily for all the electroweak observables. The

---

[*] $\alpha(m_Z^2)$ is the running QED coupling constant at $q^2 = m_Z^2$ where only the quark and lepton contributions to the deviation from its $q^2 = 0$ value, $\alpha(0) = 1/137.036$, are included. Its magnitude is commonly referred to in the literatures [29, 30, 31]. It is denoted as $\alpha(m_Z^2)_{\rm f}$ in refs. [23, 25], and is related to the coupling $\bar{\alpha}(m_Z^2)$ that contains the W-boson contribution by $1/\alpha(m_Z^2) = 1/\bar{\alpha}(m_Z^2) + 0.15$ [23, 25].

	data	SM*	pull*
LEP 1 [11]			
line-shape & FB asym.:			
m_Z (GeV)	91.1867 ± 0.0021	——	——
Γ_Z (GeV)	2.4939 ± 0.0024	2.4972	-1.4
σ_h^0(nb)	41.491 ± 0.058	41.474	0.3
R_ℓ	20.765 ± 0.026	20.747	(0.7)
$A_{\mathrm{FB}}^{0,\ell}$	0.01683 ± 0.00096	0.01651	(0.3)
for each lepton:			
R_e	20.783 ± 0.052	20.747	0.7
R_μ	20.789 ± 0.034	20.747	1.3
R_τ	20.764 ± 0.045	20.795	-0.7
$A_{\mathrm{FB}}^{0,e}$	0.0153 ± 0.0025	0.0165	-0.5
$A_{\mathrm{FB}}^{0,\mu}$	0.0164 ± 0.0013	0.0165	-0.1
$A_{\mathrm{FB}}^{0,\tau}$	0.0183 ± 0.0017	0.0165	1.1
τ polarization:			
A_τ	0.1431 ± 0.0045	0.1484	-1.2
A_e	0.1479 ± 0.0051	0.1484	-0.1
b and c quark results:			
R_b	0.21656 ± 0.00074	0.21566	1.2
R_c	0.1735 ± 0.0044	0.1721	0.3
$A_{FB}^{0,b}$	0.0990 ± 0.0021	0.1040	-2.4
$A_{FB}^{0,c}$	0.0709 ± 0.0044	0.0744	-0.8
jet charge asymmetry:			
$\sin^2\theta_{\mathrm{eff}}^{\mathrm{lept}}$	0.2321 ± 0.0010	0.2314	0.7
SLC [11]			
A_{LR}^0	0.1510 ± 0.0025	0.1484	1.0
A_b	0.867 ± 0.035	0.935	-1.9
A_c	0.647 ± 0.040	0.668	-0.5
Tevatron + LEP 2 [32]			
m_W (GeV)	80.410 ± 0.044	80.402	0.18
χ^2_{tot} (19 data points)			19.8
Parameters	**Constraints**		
m_t (GeV) [29]	173.8 ± 5.2	175.0	—
$\alpha_s(m_Z)$ [29]	0.119 ± 0.002	0.118	—
$1/\alpha(m_Z^2)$ [30]	128.90 ± 0.09	128.90	—
[31]	128.94 ± 0.04	—	—

Table 1: Electroweak measurements at LEP, SLC and Tevatron. The average W-boson mass is found in ref. [32]. The reference SM predictions and the corresponding 'pull' factors are given for $m_t = 175$ GeV, $m_{H_{\mathrm{SM}}} = 100$ GeV, $\alpha_s(m_Z) = 0.118$ and $1/\alpha(m_Z^2) = 128.90$. Correlation matrix elements of the Z line-shape parameters and those for the heavy-quark parameters are found in ref. [11]. The data R_ℓ and $A_{\mathrm{FB}}^{0,\ell}$ are obtained by assuming the e-μ-τ universality, and are not used in our χ^2 analysis.

predictions of the MSSM are then expressed as the sum of the SM predictions and the difference between the predictions of the SM and those of the MSSM. This separation is useful because the SM predictions include parts of the known two- and three-loop corrections whereas the MSSM contributions are evaluated strictly in the one-loop order in the present analysis.

2.1 Observables at Z-pole experiments

The amplitude for the decay process $Z \to f_\alpha \overline{f_\alpha}$ is written as

$$T(Z \to f_\alpha \overline{f_\alpha}) = M_\alpha^f \epsilon_Z \cdot J_{f_\alpha}, \tag{2.2}$$

where ϵ_Z^μ is the polarization vector of the Z-boson and $J_{f_\alpha}^\mu = \overline{f_\alpha}\gamma^\mu f_\alpha = \overline{f}\gamma^\mu P_\alpha f$ is the fermion current with definite chirality, $\alpha = L$ or R. The pseudo-observables of the Z-pole experiments are expressed in terms of the scalar amplitudes M_α^f with the following normalization [11]:

$$g_\alpha^f = \frac{M_\alpha^f}{\sqrt{4\sqrt{2}G_F m_Z^2}} \approx \frac{M_\alpha^f}{0.74070}. \tag{2.3}$$

A convenient parametrization of the effective couplings in generic electroweak theories has been given in refs. [24, 25]:

$$\begin{aligned}
g_L^{\nu_l} &= 0.50214 + 0.453\,\Delta\bar{g}_Z^2 + \Delta g_L^{\nu_l}, && (2.4a)\\
g_L^{l} &= -0.26941 - 0.244\,\Delta\bar{g}_Z^2 + 1.001\,\Delta\bar{s}^2 + \Delta g_L^{l}, && (2.4b)\\
g_R^{l} &= 0.23201 + 0.208\,\Delta\bar{g}_Z^2 + 1.001\,\Delta\bar{s}^2 + \Delta g_R^{l}, && (2.4c)\\
g_L^{u} &= 0.34694 + 0.314\,\Delta\bar{g}_Z^2 - 0.668\,\Delta\bar{s}^2 + \Delta g_L^{u}, && (2.4d)\\
g_R^{u} &= -0.15466 - 0.139\,\Delta\bar{g}_Z^2 - 0.668\,\Delta\bar{s}^2 + \Delta g_R^{u}, && (2.4e)\\
g_L^{d} &= -0.42451 - 0.383\,\Delta\bar{g}_Z^2 + 0.334\,\Delta\bar{s}^2 + \Delta g_L^{d}, && (2.4f)\\
g_R^{d} &= 0.07732 + 0.069\,\Delta\bar{g}_Z^2 + 0.334\,\Delta\bar{s}^2 + \Delta g_R^{d}, && (2.4g)\\
g_L^{b} &= -0.42109 - 0.383\,\Delta\bar{g}_Z^2 + 0.334\,\Delta\bar{s}^2 + \Delta g_L^{b}. && (2.4h)
\end{aligned}$$

Here the first numerical terms in the r.h.s. of the above equations are the SM predictions at the reference point, $(m_t(\mathrm{GeV}), m_{H_{\mathrm{SM}}}(\mathrm{GeV}), 1/\alpha(m_Z^2), \alpha_s(m_Z)) =$ (175, 100, 128.90, 0.118), $\Delta\bar{g}_Z^2$ and $\Delta\bar{s}^2$ are the universal gauge-boson-propagator corrections [23], and Δg_α^f ($\alpha = L, R$) are the process specific corrections. In the SM the following universality relations hold very accurately:

$$\begin{aligned}
(\Delta g_L^{\nu_e})_{\mathrm{SM}} &= (\Delta g_L^{\nu_\mu})_{\mathrm{SM}} = (\Delta g_L^{\nu_\tau})_{\mathrm{SM}} = 0, && (2.5a)\\
(\Delta g_\alpha^{e})_{\mathrm{SM}} &= (\Delta g_\alpha^{\mu})_{\mathrm{SM}} = (\Delta g_\alpha^{\tau})_{\mathrm{SM}} = 0, && (2.5b)\\
(\Delta g_\alpha^{u})_{\mathrm{SM}} &= (\Delta g_\alpha^{c})_{\mathrm{SM}} = 0, && (2.5c)\\
(\Delta g_R^{d})_{\mathrm{SM}} &= (\Delta g_R^{s})_{\mathrm{SM}} = (\Delta g_R^{b})_{\mathrm{SM}} = 0, && (2.5d)\\
(\Delta g_L^{d})_{\mathrm{SM}} &= (\Delta g_L^{s})_{\mathrm{SM}} = 0 \neq (\Delta g_L^{b})_{\mathrm{SM}}. && (2.5e)
\end{aligned}$$

Only the term $(\Delta g_L^b)_{\rm SM}$ has non-trivial m_t and $m_{H_{\rm SM}}$ dependence. In the MSSM, we find that all the (Δg_α^f) terms are non-vanishing, and the flavor-universality holds only among the first two generations. We study $\Delta g_L^{\nu_\tau}, \Delta g_L^\tau, \Delta g_R^\tau, \Delta g_L^b$ and Δg_R^b separately in the following sections.

The universal part of the corrections $\Delta \bar{g}_Z^2$ and $\Delta \bar{s}^2$ are defined as the shift in the effective couplings $\bar{g}_Z^2(m_Z^2)$ and $\bar{s}^2(m_Z^2)$ [23] from their SM reference values at $(m_t({\rm GeV}), m_{H_{\rm SM}}({\rm GeV}), 1/\alpha(m_Z^2)) =$ (175, 100, 128.90):

$$\bar{g}_Z^2(m_Z^2) = 0.55635 + \Delta \bar{g}_Z^2, \tag{2.6a}$$

$$\bar{s}^2(m_Z^2) = 0.23035 + \Delta \bar{s}^2. \tag{2.6b}$$

We find it convenient to express the above shifts in the two effective couplings in terms of the two parameters ΔS_Z and ΔT_Z,

$$\Delta \bar{g}_Z^2 = 0.00412 \Delta T_Z, \tag{2.7a}$$

$$\Delta \bar{s}^2 = 0.00360 \Delta S_Z - 0.00241 \Delta T_Z. \tag{2.7b}$$

The parameters S_Z and T_Z are related to the S and T parameters [19]

$$S_Z \equiv S + R - 0.064 x_\alpha, \tag{2.8a}$$

$$T_Z \equiv T + 1.49 R - \frac{\Delta \overline{\delta}_G}{\alpha}, \tag{2.8b}$$

in the notation of refs. [23, 24, 25]. A compact summary of the definitions of the effective charges of ref. [23] and the oblique parameters S, T, U, R are given in Appendix B. The shift R

$$\frac{4\pi}{\bar{g}_Z^2(m_Z^2)} - \frac{4\pi}{\bar{g}_Z^2(0)} \equiv -\frac{1}{4} R = -\frac{1}{4}(1.1879 + \Delta R), \tag{2.9}$$

accounts for the difference between the T parameter which measures the neutral current strength at the zero-momentum transfer [19, 33] and the T_Z parameter which measures the quantity on the Z-pole. The x_α-dependent term in S_Z reflects the fact that only a combination of S and $1/\alpha(m_Z^2)$ is constrained by the Z-pole asymmetry experiments [23, 25, 34]. The factor $\overline{\delta}_G$ denotes the vertex and box corrections to the muon decay constant

$$G_F = \frac{\bar{g}_W^2(0) + \hat{g}^2 \overline{\delta}_G}{4\sqrt{2} m_W^2}, \tag{2.10}$$

which takes $\overline{\delta}_G = 0.0055$ [23] in the SM. In the MSSM, vertex and box corrections affect its magnitude and we define the shift $\Delta \overline{\delta}_G$ as

$$\overline{\delta}_G = 0.00550 + \Delta \overline{\delta}_G. \tag{2.11}$$

Although the supersymmetric contribution to $\Delta\bar{\delta}_G$ is the correction specific to the muon decay rather than a part of the universal gauge-boson-propagator corrections, it appears in all the predictions of the electroweak observables because we use the muon decay constant G_F as one of the basic inputs of our calculations. We therefore include the effect $\Delta\bar{\delta}_G$ as a part of our "universal" parameter, T_Z.

By inserting (2.9) into (2.8) and by using the shifts ΔS and ΔT [23] from the reference SM values of the S and T parameters, we can express the parameters ΔS_Z and ΔT_Z as

$$\Delta S_Z = S_Z - 0.955 = \Delta S + \Delta R - 0.064 x_\alpha, \tag{2.12a}$$

$$\Delta T_Z = T_Z - 2.65 \quad = \Delta T + 1.49 \Delta R - \frac{\Delta\bar{\delta}_G}{\alpha}. \tag{2.12b}$$

The SM contribution to the shift $\Delta S, \Delta T$ and ΔR are parametrized as [23, 24]

$$(\Delta S)_{\rm SM} = -0.007 x_t + 0.091 x_h - 0.010 x_h^2, \tag{2.13a}$$

$$\begin{aligned}(\Delta T)_{\rm SM} = {} & (0.130 - 0.003 x_h) x_t + 0.003 x_t^2 - 0.079 x_h - 0.028 x_h^2 \\ & + 0.0026 x_h^3,\end{aligned} \tag{2.13b}$$

$$(\Delta R)_{\rm SM} = -0.124 \left\{ \log\left[1 + \left(\frac{26}{m_{H_{\rm SM}}({\rm GeV})}\right)^2\right] - \log\left[1 + \left(\frac{26}{100}\right)^2\right] \right\}, \tag{2.13c}$$

and we set $(\Delta\bar{\delta}_G)_{\rm SM} = 0$ in our calculation. The explicit form of the MSSM contributions to the parameters $\Delta S, \Delta T, \Delta R$ are given in Appendix B. The MSSM contributions to the muon-decay parameter $\Delta\bar{\delta}_G$ is given in Appendix D, and those to the effective Z-boson decay amplitudes, Δg_α^f, are given in Appendix C.

The pseudo-observables of the Z-pole experiments are then obtained by using the above 12 effective couplings g_α^f; 8 couplings of eq. (2.4) that are distinct in the SM, and the 4 additional coupling, $g_L^{\nu_\tau}$, g_L^τ, g_R^τ and g_R^b, which can be distinct in the MSSM. The partial widths of the Z-boson are

$$\Gamma_f = \frac{G_F m_Z^3}{3\sqrt{2}\pi} \left\{ \left| g_L^f + g_R^f \right|^2 \frac{C_{fV}}{2} + \left| g_L^f - g_R^f \right|^2 \frac{C_{fA}}{2} \right\} \left(1 + \frac{3}{4} Q_f^2 \frac{\alpha(m_Z^2)}{\pi} \right), \tag{2.14}$$

where the factors C_{fV} and C_{fA} account for the final state mass and QCD corrections for quarks. Their numerical values are listed in Table 2. The α_s-dependence in C_{qV}, C_{qA} is parametrized in terms of the parameter x_s (2.1d). The last term proportional to $\alpha(m_Z^2)/\pi$ in eq. (2.14) accounts for the final state QED correction. The total decay width Γ_Z and the hadronic decay width Γ_h are given in terms of the partial width Γ_f:

$$\Gamma_Z = 3\Gamma_\nu + \Gamma_e + \Gamma_\mu + \Gamma_\tau + \Gamma_h, \tag{2.15a}$$

$$\Gamma_h = \Gamma_u + \Gamma_c + \Gamma_d + \Gamma_s + \Gamma_b. \tag{2.15b}$$

	C_{fV}	C_{fA}
u	$3.1166 + 0.0030x_s$	$3.1351 + 0.0040x_s$
$d = s$	$3.1166 + 0.0030x_s$	$3.0981 + 0.0021x_s$
c	$3.1167 + 0.0030x_s$	$3.1343 + 0.0041x_s$
b	$3.1185 + 0.0030x_s$	$3.0776 + 0.0030x_s$
ν	1	1
$e = \mu$	1	1
τ	1	0.9977

Table 2: Numerical values of factors C_{fV}, C_{fA} for quarks and leptons used in eq. (2.14).

The ratios R_l, R_c, R_b and the hadronic peak cross section σ_h^0 are given by:

$$R_l = \frac{\Gamma_h}{\Gamma_l},\ R_c = \frac{\Gamma_c}{\Gamma_h},\ R_b = \frac{\Gamma_b}{\Gamma_h},\ \sigma_h^0 = \frac{12\pi}{m_Z^2}\frac{\Gamma_e\Gamma_h}{\Gamma_Z^2}, \tag{2.16}$$

where $l = e, \mu$ or τ.

The left-right asymmetry parameter A^f is also given in terms of the effective couplings g_α^f as

$$A^f = \frac{(g_L^f)^2 - (g_R^f)^2}{(g_L^f)^2 + (g_R^f)^2}. \tag{2.17}$$

The forward-backward (FB) asymmetry $A_{FB}^{0,f}$ and the left-right (LR) asymmetry A_{LR}^0 are then expressed as follows:

$$A_{FB}^{0,f} = \frac{3}{4}A^e A^f, \tag{2.18a}$$

$$A_{LR}^0 = A^e. \tag{2.18b}$$

The effective parameter $\sin^2\theta_{\text{eff}}^{\text{lept}}$ measured from the jet-charge FB asymmetry is defined as

$$\sin^2\theta_{\text{eff}}^{\text{lept}} = \frac{1}{2}\frac{g_R^e}{g_R^e - g_L^e}. \tag{2.19}$$

All the Z-boson parameters in Table 1 are now calculable for arbitrary values of $m_t, m_{H_{\text{SM}}}, \alpha(m_Z^2)$ and $\alpha_s(m_Z)$, or x_t, x_h, x_α and x_s, respectively, in the SM by using the parametrizations given in this section. The predictions of the MSSM are calculated by using the formulae in Appendices B, C and D, by using the mixing matrix and the coupling notation [28] of Appendix A.

2.2 The W-boson mass

The theoretical prediction of m_W can be parametrized as [23, 24]

$$\begin{aligned} m_W(\mathrm{GeV}) &= 80.402 + \Delta m_W, & (2.20a)\\ \Delta m_W(\mathrm{GeV}) &= -0.288\Delta S + 0.418\Delta T + 0.337\Delta U \\ &\qquad + 0.012 x_\alpha - 0.126\frac{\Delta\bar{\delta}_G}{\alpha}. & (2.20b)\end{aligned}$$

Here in addition to the S and T parameters, the U parameter [19] is needed to calculate the effective charge $\bar{g}_W^2(0)$ [23] that determines the muon decay constant G_F; see eq. (2.10). The SM contribution to the shift Δm_W from the reference prediction can be parametrized as [24, 25]

$$\begin{aligned}(\Delta m_W)_{\mathrm{SM}} &= 0.064x_t - 0.060x_h - 0.009x_h^2 + 0.001x_t(x_t - x_h) \\ &\quad +0.001x_h^3 + 0.012x_\alpha, \qquad (2.21)\end{aligned}$$

which is obtained by inserting the SM contributions to $\Delta S, \Delta T$ and ΔU [24, 25] to eq. (2.20b). The MSSM gives additional contributions to S, T, U and to $\Delta\bar{\delta}_G$:

$$\Delta m_W = (\Delta m_W)_{\mathrm{SM}} - 0.288S_{\mathrm{new}} + 0.418T_{\mathrm{new}} + 0.337U_{\mathrm{new}} - 0.126\frac{\Delta\bar{\delta}_G}{\alpha}, \qquad (2.22)$$

where

$$S_{\mathrm{new}} = \Delta S - (\Delta S)_{\mathrm{SM}}, \quad T_{\mathrm{new}} = \Delta T - (\Delta T)_{\mathrm{SM}}, \quad U_{\mathrm{new}} = \Delta U - (\Delta U)_{\mathrm{SM}}. \qquad (2.23)$$

The MSSM contribution to S_{new}, T_{new}, U_{new} and $\Delta\bar{\delta}_G$ are given in appendices B and D.

2.3 Constraints on $m_t, \alpha(m_Z^2)$ and $\alpha_s(m_Z)$, and the SM fit

All the electroweak observables are now calculated in the SM as functions of the four parameters, $m_t, m_{H_{\mathrm{SM}}}, \alpha(m_Z^2)$ and $\alpha_s(m_Z)$, or x_t, x_h, x_α and x_s, respectively via (2.1). The Higgs boson has not been found yet and the lower mass bound

$$m_{H_{\mathrm{SM}}}(\mathrm{GeV}) \gtrsim 90 \qquad (x_h \gtrsim -0.11), \qquad (2.24)$$

is obtained from the LEP2 experiment [35].

In our analysis we use the following constraints on the parameters m_t [29], $\alpha_s(m_Z)$ [29] and $\alpha(m_Z^2)$ [30]

$$\begin{aligned} m_t(\mathrm{GeV}) &= 173.8 \pm 5.2 & (x_t = -0.12 \pm 0.52), && (2.25a)\\ 1/\alpha(m_Z^2) &= 128.90 \pm 0.09 & (x_\alpha = 0 \pm 1), && (2.25b)\\ \alpha_s(m_Z) &= 0.119 \pm 0.002 & (x_s = 0.33 \pm 0.67), && (2.25c)\end{aligned}$$

as shown in the bottom of Table 1. As an alternative to the model-independent estimate (2.25b) [30], we also examine the case with the estimate [31]:

$$1/\alpha(m_Z^2) = 128.94 \pm 0.04 \quad (x_\alpha = 0.44 \pm 0.44), \tag{2.26}$$

which is obtained by using the perturbative QCD constraints down to the τ-lepton mass scale.

We find that the reference point of our analysis ($x_t = x_h = x_\alpha = x_s = 0$) is not far from the global minimum of the SM fit. With the external constraints of eq. (2.25), we find $\chi^2_{\rm min}/(\text{d.o.f.}) = 18.2/(22-4)$ at

$$m_t(\text{GeV}) = 172.3 \pm 5.0, \tag{2.27a}$$
$$\alpha_s(m_Z) = 0.119 \pm 0.002, \tag{2.27b}$$
$$1/\alpha(m_Z^2) = 128.90 \pm 0.09, \tag{2.27c}$$
$$m_{H_{\rm SM}}(\text{GeV}) = 117^{+98}_{-64}. \tag{2.27d}$$

By replacing the estimate (2.25b) [30] by (2.26) [31], we find $\chi^2_{\rm min}/(\text{d.o.f.}) = 18.3/(22-4)$ at

$$m_t(\text{GeV}) = 172.6 \pm 4.9, \tag{2.28a}$$
$$\alpha_s(m_Z) = 0.119 \pm 0.002, \tag{2.28b}$$
$$1/\alpha(m_Z^2) = 128.94 \pm 0.04, \tag{2.28c}$$
$$m_{H_{\rm SM}}(\text{GeV}) = 144^{+88}_{-58}. \tag{2.28d}$$

In summary, the SM gives a good fit to all the electroweak data if the Higgs boson mass is relatively light, with the mass below a few hundred GeV, as suggested by the ranges (2.27d) or (2.28d).

3 The minimal supersymmetric standard model (MSSM)

In subsection 3.1 we briefly summarize the MSSM and our coupling conventions. In subsection 3.2, we summarize the constraints on supersymmetric particle masses from direct search experiments.

3.1 The MSSM Lagrangian

We study consequences of the MSSM under the following constraints.

(i) It has the minimal particle content, with the gauginos of the $\text{SU}(3)_C$, $\text{SU}(2)_L$ and $\text{U}(1)_Y$ groups, three generations of squarks and sleptons, and two pairs of Higgs doublets and their superpartners.

(ii) It has the minimal superpotential, which is sufficient to give masses to all the quarks and leptons. In particular, we do not consider R-parity non-conserving interactions.

(iii) The three gaugino masses, M_3, M_2, M_1 are taken to be independent, while most of our numerical results are obtained under the 'unification' condition, $M_3/M_2/M_1 = \hat{\alpha}_3(m_Z)/\hat{\alpha}_2(m_Z)/\hat{\alpha}_1(m_Z)$, where $\hat{\alpha}_i(\mu)$ are the $\overline{\rm MS}$ couplings.

(iv) The scalar masses are introduced in such a way that squark and slepton interactions with neutralinos and gluinos are flavor conserving in the basis where quarks and leptons have definite mass.

(v) The scalar masses of the first two generations are taken to be equal. We therefore have 5 scalar masses for the first two generations, and another 5 for the third generation squarks and sleptons.

(vi) We neglect mixings between the left- and right-chirality sfermions in the first two generations. Accordingly, we retain the soft SUSY breaking A parameters only in the third generations, A_t, A_b and A_τ.

Under the above constraints, the MSSM interactions can be parameterized in terms of 19 parameters: the ratio of the two v.e.v.'s $\tan\beta$, the Higgs-mixing mass μ, the pseudo-scalar Higgs-boson mass m_A, the three gaugino masses M_3, M_2, M_1, the three A parameters A_t, A_b, A_τ, the five sfermion masses for the first two generations, $m_{\widetilde{Q}}$, $m_{\widetilde{U}}$, $m_{\widetilde{D}}$, $m_{\widetilde{L}}$, $m_{\widetilde{E}}$, and the five sfermion for the third generations, $m_{\widetilde{Q}_3}, m_{\widetilde{U}_3}, m_{\widetilde{D}_3}, m_{\widetilde{L}_3}, m_{\widetilde{E}_3}$. Summing up, the 19 parameters of our MSSM Lagrangian are

$$\tan\beta, \mu, m_A, \tag{3.1a}$$

$$M_3, M_2, M_1, \tag{3.1b}$$

$$A_t, A_b, A_\tau, \tag{3.1c}$$

$$m_{\widetilde{Q}}, m_{\widetilde{U}}, m_{\widetilde{D}}, m_{\widetilde{L}}, m_{\widetilde{E}}, \tag{3.1d}$$

$$m_{\widetilde{Q}_3}, m_{\widetilde{U}_3}, m_{\widetilde{D}_3}, m_{\widetilde{L}_3}, m_{\widetilde{E}_3}. \tag{3.1e}$$

All our analytic expressions are valid when the above 19 parameters of the MSSM are independently varied. Because the parameter space of the MSSM is too large even with the above restrictions, we present our numerical results often by varying only the few most relevant parameters while keeping the rest of the parameters fixed at some appropriate values. Systematic investigation of the parameter space of the two representative models, the supergravity mediated and the gauge-interaction mediated supersymmetry breaking models, will be reported elsewhere [27].

The MSSM Lagrangian with the above constraints are adopted for the new Feynman amplitude generator MadGraph2 [36], and its explicit form can be found in ref. [28]. A compact summary of our notation is given in Appendix A. All the physical masses and couplings of the supersymmetric particles are calculated in the tree-level by using the MSSM Lagrangian with the above restrictions.

We denote the two chargino mass eigenstates as, $\widetilde{\chi}_i^-$ with $m_{\widetilde{\chi}_1^-} < m_{\widetilde{\chi}_2^-}$, the four neutralinos as, $\widetilde{\chi}_i^0$, with $m_{\widetilde{\chi}_1^0} < \cdots < m_{\widetilde{\chi}_4^0}$, and the gluino as $\widetilde{g}$. The 7 sfermion mass eigenstates for each generation are denoted by, $\widetilde{u}_L, \widetilde{d}_L, \widetilde{u}_R, \widetilde{d}_R, \widetilde{\nu}_l, \widetilde{l}_L, \widetilde{l}_R$ for the first two generations, and $\widetilde{t}_1, \widetilde{t}_2, \widetilde{b}_1, \widetilde{b}_2, \widetilde{\nu}_\tau, \widetilde{\tau}_1, \widetilde{\tau}_2$ for the third generation. The four Higgs boson mass eigenstates, the light and heavy CP-even neutral Higgs bosons h and H ($m_h < m_H$), the CP-odd neutral Higgs boson A, and the charged Higgs boson $H^\pm$ are obtained by using the improved effective potential of ref. [12] that assumes CP invariance[†].

A few comments are in order. Although we do not consider models with non-minimal interactions, such as the R-parity violating models or models with gauge interaction mediated supersymmetry breaking where the very light gravitino becomes the lightest supersymmetric particle (LSP), all our results should be valid in those models with additional interactions, as long as their strengths are negligibly small as compared to the gauge interactions. Our analytic expressions allow for arbitrary CP violating phases in the mass parameters, μ and A_f, and hence some of the couplings have associated complex phases. Our numerical results are, however, given in the CP conserving limit of the MSSM interactions. This is mainly because we adopt the effective Higgs potential of ref. [12] that assumes CP invariance in the scalar sector. Effects of CP violating interactions in the MSSM will be reported elsewhere.

3.2 Bounds on the masses of SUSY particles from the direct search

The predictions of the MSSM for all the electroweak observables reduce to those of the SM with the restricted Higgs boson mass range, $m_h \lesssim 135$ GeV [12, 14, 15, 16], in the limit where all the supersymmetry breaking mass parameters are large. In the following analysis, we explicitly demonstrate this decoupling behavior quantitatively for all the electroweak observables.

The differences between the predictions of the SM and those of the MSSM are hence largest when the supersymmetric particle masses are near their present lower bounds from the direct search experiments. We calculate the particle masses from the 19 parameters of the MSSM, eq. (3.1), and confront them with those lower mass bounds.

[†] The radiative corrections beyond the 1-loop level on the lightest Higgs boson mass have been discussed in refs. [14, 15, 16]. Those effects shift the theoretical prediction on m_h in the leading order a few GeV. Since the result of our analysis, however, is not affected quantitatively by such a small shift of m_h, we take into account the leading order correction on m_h in our study for brevity.

Current limits on the masses of scalar leptons are obtained from the LEP2 experiments as [37]

$$m_{\widetilde{e}_R} \gtrsim 88 \text{ GeV}, \tag{3.2a}$$

$$m_{\widetilde{\mu}_R} \gtrsim 80 \text{ GeV}, \tag{3.2b}$$

$$m_{\widetilde{\tau}_R} \gtrsim 69 \text{ GeV}, \tag{3.2c}$$

where $\widetilde{\tau}_R$ has been assumed to be the mass eigenstate. The corresponding limits for the chirality-left sleptons are weaker and depend on the mass of the charginos. The lower mass bounds for scalar quarks and gluinos are obtained from the Tevatron search experiments as [38]

$$m_{\widetilde{q}} \gtrsim 212 \text{ GeV}, \tag{3.3a}$$

$$m_{\widetilde{g}} \gtrsim 173 \text{ GeV}, \tag{3.3b}$$

when the squark masses are common for the 5 light flavors and both chiralities, and when either the squarks or the gluino are much heavier. The bounds on squark masses depend, however, on details of their mass spectrum and on their decay patterns. The (almost) model-independent lower mass bounds are found from the LEP2 experiments [37]:

$$m_{\widetilde{t}_1} \gtrsim 88 \text{ GeV}, \tag{3.4a}$$

$$m_{\widetilde{b}_1} \gtrsim 76 \text{ GeV}. \tag{3.4b}$$

For charginos and neutralinos the following bounds are found from the LEP2 experiments [37]:

$$m_{\widetilde{\chi}^0_1} \gtrsim 33 \text{ GeV}, \tag{3.5a}$$

$$m_{\widetilde{\chi}^-_1} \gtrsim 90 \text{ GeV}. \tag{3.5b}$$

Those on the Higgs particles are [35]

$$m_{H_{\text{SM}}} > 95 \text{ GeV}, \tag{3.6a}$$

$$m_h \gtrsim 84 \text{ GeV}, \tag{3.6b}$$

$$m_A \gtrsim 85 \text{ GeV}, \tag{3.6c}$$

$$m_{H^-} \gtrsim 69 \text{ GeV}. \tag{3.6d}$$

In addition, for the neutral particles, we assume

$$m_{\widetilde{\nu}} > 45 \text{ GeV}, \tag{3.7a}$$

$$m_{\widetilde{\chi}^0_1} + m_{\widetilde{\chi}^0_2} > m_Z, \tag{3.7b}$$

so that they do not contribute to the total width of the Z-boson [11].

4 Oblique corrections in the MSSM

As explained in the introduction, the MSSM contributions to the vertex or box corrections vanish whenever either the sypersymmetric scalars (squarks and sleptons) or the supersymmetric fermions (charginos, neutralinos, and the gluino) are heavy enough. In those cases, the MSSM particles can still affect the electroweak observables via their contributions to the gauge-boson propagators, which are often called the *oblique* corrections [19, 20, 21, 22]. Because the oblique corrections affect all the electroweak observables in a flavor-independent manner (universality), and because their effects are found to be most significant under the present constraints on the new particle masses as summarized in the previous section, we study them in this section in great detail.

The formalism presented in section 2 tells us that the precision electroweak experiments at the Z-boson pole constrain just two oblique parameters, S_Z and T_Z, whereas the W-boson mass m_W can be taken as the third oblique parameter. We favor m_W over the U parameter as our third oblique parameter, because we can avoid correlations among the three oblique parameters this way and because we could not gain insight by adopting the U parameter in our MSSM analysis.

In the following subsections, we examine the oblique corrections from each sector of the MSSM, since all the oblique corrections are expressed as linear sum of individual contributions [26]: squarks and sleptons (sec. 4.1), the MSSM Higgs bosons (sec. 4.2), and charginos and neutralinos (sec. 4.3). The effects of combining all the contributions are discussed in subsection 4.4. As remarked above, the dominance of the oblique contributions to the electroweak observables is justified only when either the sfermions or the supersymmetric (-ino) fermions are heavy. All the oblique contributions are of course relevant always as a part of the full MSSM contributions.

In presenting our results, we find it most convenient to parameterize first the experimental constraints on the oblique parameters, and then confront the MSSM contributions to those parameters against the experimental constraints. We further observe that the uncertainty in the SM contributions to the oblique parameters which arise from the uncertainty in $m_{H_{\rm SM}}$ (2.24), m_t (2.25a) and $\alpha(m_Z^2)$, (2.25b) or (2.26), is significant as compared to the magnitudes of the MSSM contributions. The uncertainty in $\alpha_s(m_Z)$ (2.25c) has been found to affect our results little. We therefore obtain the constraints on the oblique parameters in such a way that we can examine the sum of the SM and the MSSM contributions for arbitrary values of $m_t, m_{H_{\rm SM}}$ and $\alpha(m_Z^2)$ within their present constraints. This can be achieved by observing that the m_t and $m_{H_{\rm SM}}$ dependences of the SM predictions appear only in the oblique parameters and in the Zb_Lb_L vertex correction, Δg_L^b, and by observing that their $\alpha(m_Z^2)$ dependences appear only through the combination S_Z (2.12a)

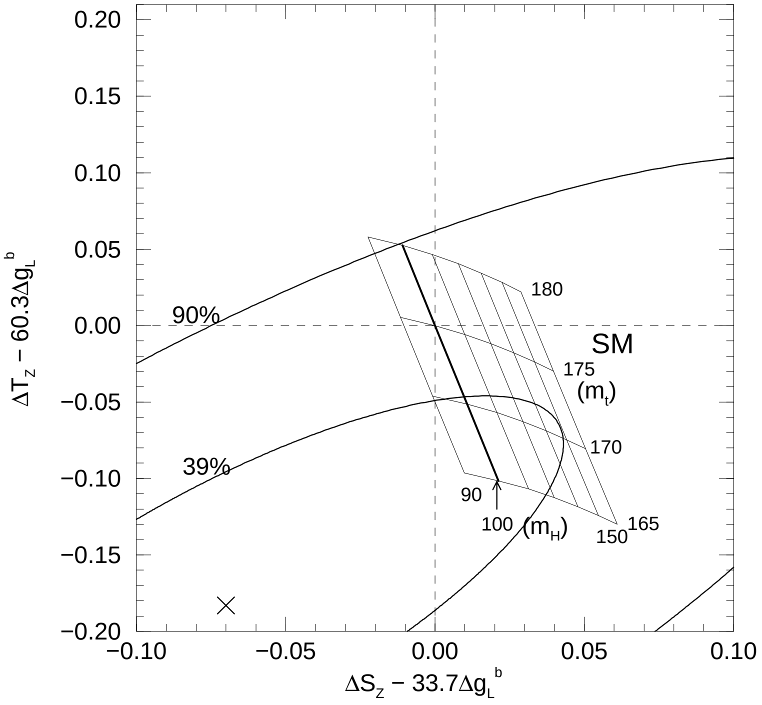

Figure 1: Constraints on $\Delta S_Z - 33.7\Delta g_L^b$ and $\Delta T_Z - 60.3\Delta g_L^b$ from the electroweak precision measurements. The symbol (×) denotes the best fit from the electroweak data. The 39% ($\Delta\chi^2 = 1$) and 90% ($\Delta\chi^2 = 4.61$) contours are shown. The SM predictions are given for $m_t = 165 \sim 180$ GeV and $m_{H_{\rm SM}} = 90 \sim 150$ GeV.

and Δm_W (2.20b).

By adopting the 5 parameters, $\Delta S_Z, \Delta T_Z, \Delta g_L^b, \Delta m_W$ and $\alpha_s(m_Z)$ as the free adjustable parameters, we find the following fit for all the electroweak observables of Table 1, under the constraint (2.25c):

$$\left.\begin{array}{rcl} \Delta S_Z - 33.7\Delta g_L^b & = & -0.070 \pm 0.113 \\ \Delta T_Z - 60.3\Delta g_L^b & = & -0.183 \pm 0.137 \end{array}\right\}, \qquad \rho = 0.89, \tag{4.1a}$$

$$\Delta m_W(\text{ GeV}) = \quad 0.008 \pm 0.046, \tag{4.1b}$$

$$\chi^2_{\rm min} = 15.4 + \left(\frac{\Delta g_L^b + 0.00086}{0.00076}\right)^2, \tag{4.1c}$$

where d.o.f.$= 20 - 5 = 15$.

The results of the fit are shown in Figs. 1 and 2, where the SM predictions for some representative values of m_t and $m_{H_{\rm SM}}$ are given for $1/\alpha(m_Z^2) = 128.90$ ($x_\alpha = 0$) [30]. The predictions for different estimate of $1/\alpha(m_Z^2)$ can easily be obtained by using the x_α-dependences of ΔS_Z (2.12a) and Δm_W (2.20b). Fig. 1 shows the constraint (4.1a) in the plane of $\Delta S_Z - 33.7\Delta g_L^b$ and $\Delta T_Z - 60.3\Delta g_L^b$. It is clearly seen from this figure that relatively low value of m_t as compared to

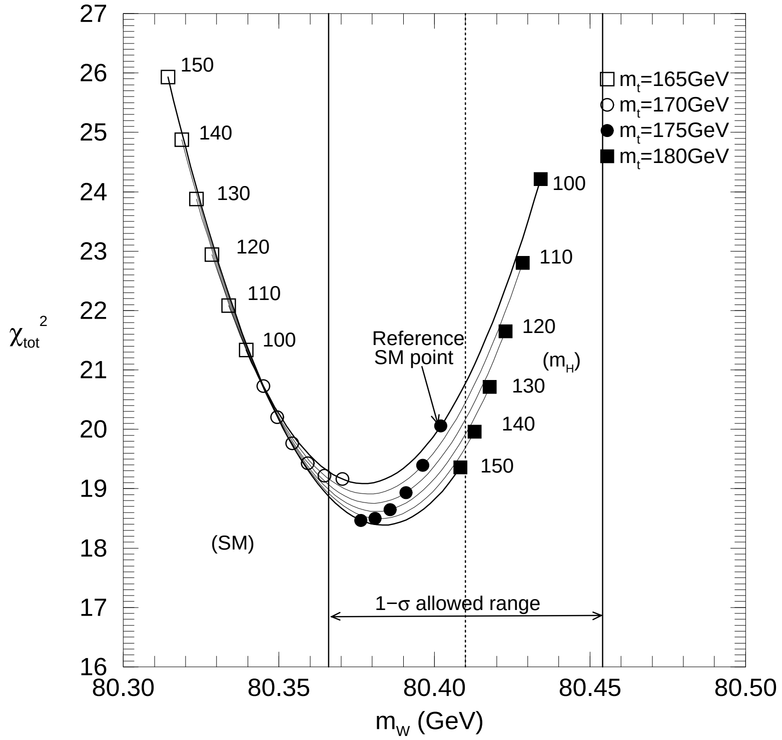

Figure 2: The total χ^2 versus m_W. The 1-σ experimental bound on m_W is shown. The SM predictions are given for $m_t = 165 \sim 180$ GeV and $m_{H_{\rm SM}} = 100 \sim 150$ GeV. The reference SM point at $m_t = 175$ GeV, $m_{H_{\rm SM}} = 100$ GeV, $1/\alpha(m_Z^2) = 128.90$ is shown by the arrow.

the present experimental mean value (2.25a) and relatively light Higgs boson are favored within the SM fit. In Fig. 2, the SM prediction for m_W (at $x_\alpha = 0$) and the resulting total χ^2 are shown. The m_W data slightly favors $m_{H_{\rm SM}} = 100$ GeV over $m_{H_{\rm SM}} = 150$ GeV for $m_t \lesssim 170$ GeV, so does the total χ^2. When $m_t \gtrsim 175$ GeV, the trend is reversed and $m_{H_{\rm SM}} = 150$ GeV is favored against $m_{H_{\rm SM}} = 100$ GeV in the total χ^2.[‡]

The SM fits reported in section 2, eqs. (2.27) and (2.28), are obtained from the above fit by combining it with the constraint on m_t (2.25a), and that on $1/\alpha(m_Z^2)$, (2.25b) or (2.26), respectively. In both Figs. 1 and 2, the theoretical predictions are given for the reference value of $1/\alpha(m_Z^2) = 128.90$, or $x_\alpha = 0$, in eq. (2.1c). Effects of changing $1/\alpha(m_Z^2)$ can easily be studied by shifting the theoretical predictions shown for $x_\alpha = 0$ by

---

[‡] The $\chi^2_{\rm tot}$ value in the figures 2, 4, 7 for the SM reference point at $m_t = 175$ GeV and $m_{H_{\rm SM}} = 100$ GeV is about 0.25 larger than the quoted value of 19.8 in Table 1, because of the contribution from the $\alpha_s(m_Z)$ constraint (2.25c).

$$\Delta S_Z(x_\alpha = 0) \to \Delta S_Z(x_\alpha = 0) - 0.064 x_\alpha \,, \tag{4.2a}$$

$$\Delta m_W(x_\alpha = 0) \to \Delta m_W(x_\alpha = 0) + 0.012 x_\alpha \,, \tag{4.2b}$$

as required by eqs.(2.12a) and (2.20b). Change in $1/\alpha(m_Z^2)$ of the full uncertainty of the conservative estimate (2.25b) makes $x_\alpha = \pm 1$ in eq. (2.1c). We can clearly see from Fig. 1 that the resulting horizontal shift of the SM prediction due to eq.(4.2a) can affect significantly the preferred range of the Higgs boson mass in the SM. Inspection of Fig. 2 with the shift due to eq. (4.2b) tells us that the effect is not significant for m_W with its present measurement error. We can verify the effect by comparing the SM fits (2.27) and (2.28), that were obtained by using the two estimates, (2.25b) and (2.26), respectively. The mean value of the estimate (2.26) is about $x_\alpha = 0.4$, and hence the SM prediction in Fig. 1 moves horizontally in the negative direction by about 0.03. This may affect the Higgs boson mass by about 30%. Although naive, this simple estimate reproduces qualitatively the difference in the most favored value of $m_{H_{\rm SM}}$ in the two fits, that are found to be about 22% between eqs.(2.27) and (2.28).

In the following subsections, we show the MSSM contributions to the oblique parameters by superposing them on Figs. 1 and 2, by choosing the reference SM point at $m_t = 175$ GeV and $m_{H_{\rm SM}} = 100$ GeV ($x_t = x_h = 0$). The MSSM predictions for other choices of m_t and $m_{H_{\rm SM}}$ are then obtained simply by shifting the SM reference point.

4.1 Squarks and sleptons

In Fig. 3 we show the sfermion contributions to ΔS_Z and ΔT_Z that are superposed to the SM contribution of Fig. 1. The origin of the plot ($\Delta S_Z = \Delta T_Z = \Delta g_L^b = 0$), marked by the big open circle, gives the SM prediction at $m_t = 175$ GeV and $m_{H_{\rm SM}} = 100$ GeV for $1/\alpha(m_Z^2) = 128.90$ ($x_\alpha = 0$). The contributions of the squarks and sleptons are shown separately. The net result should be obtained by adding the SM contribution, the squark contribution and the slepton contribution vectorially in the two-dimensional plot.

It is clear from the figure that for $m_t \sim 175$ GeV and $m_{H_{\rm SM}} \lesssim 130$ GeV, both the squark and slepton contributions make the fit worse than the SM. The situation does not improve by changing our estimate for $1/\alpha(m_Z^2)$ in the range (2.25b). The squark contribution makes the fit worse, because it always makes T_Z larger than the SM prediction, which is already larger than the preferred value of the data. The slepton contribution makes the fit worse, because it gives negative S_Z with either $T_Z = 0$ ($\tan\beta = 2$) or with slightly positive T_Z ($\tan\beta = 50$). The better

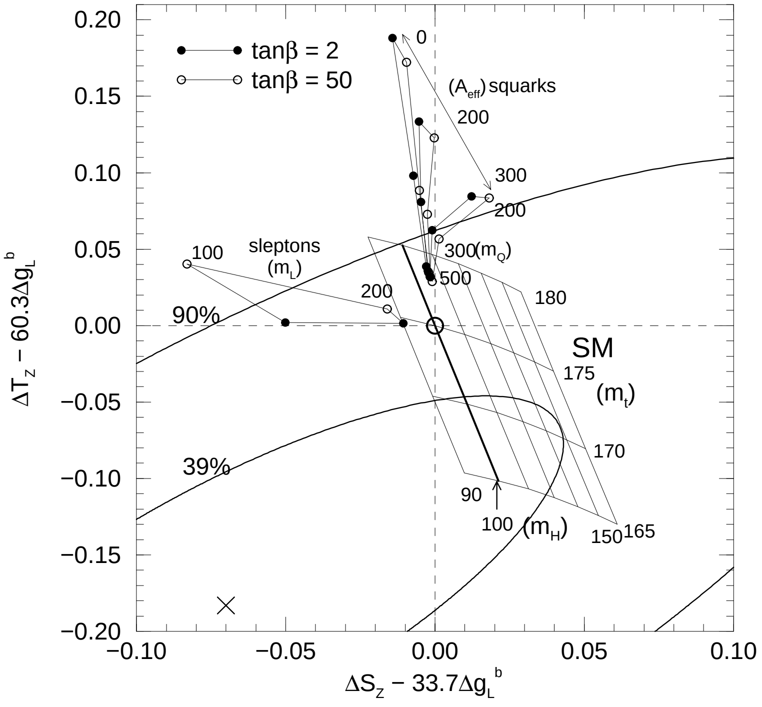

Figure 3: The squark and slepton contributions to $(\Delta S_Z, \Delta T_Z)$ for $\tan\beta = 2$ and 50. The SUSY breaking scalar masses for the left-handed and right-handed squarks are assumed to be same, denoted by $m_{\widetilde{Q}}$. The $\widetilde{t}_L$-$\widetilde{t}_R$ and $\widetilde{b}_L$-$\widetilde{b}_R$ mixings are controlled by $A_{\rm eff} = A^t_{\rm eff} = A^b_{\rm eff}$. In the slepton sector, although sizable $\widetilde{\tau}_L$-$\widetilde{\tau}_R$ mixing may be induced for large $\tan\beta$, the mixing is neglected because it does not affect both ΔS_Z and ΔT_Z significantly. The reference SM point ($\Delta S_Z = \Delta T_Z = \Delta g^b_L = 0$) is marked by the open circle at the origin.

fit to the data requires a contribution with *both* $\Delta S_Z < 0$ *and* $\Delta T_Z < 0$, which cannot be achieved by the contributions from squarks and sleptons.

Let us examine the squark and slepton contributions to the ΔS_Z and ΔT_Z parameters in more detail. We find that they do not contribute significantly to R, and hence we can understand the qualitative behavior by studying their contribution to S and T. To fix our notation, we first give the squared mass matrix of the squarks and sleptons. Since the structure of the mass matrix of sfermions are similar among the different flavors, we give the mass-squared matrix of the stop as an example. In the $(\widetilde{t}_L, \widetilde{t}_R)$ basis it is given by

$$M^2_{\widetilde{t}} = \begin{pmatrix} m^2_{\widetilde{t}_L} & m_t (A^t_{\rm eff})^* \\ m_t A^t_{\rm eff} & m^2_{\widetilde{t}_R} \end{pmatrix}, \tag{4.3a}$$

$$m^2_{\widetilde{t}_L} = m^2_{\widetilde{Q}_3} + m_Z^2 \cos 2\beta (I_{3u} - \hat{s}^2 Q_u) + m_t^2, \tag{4.3b}$$

$$m^2_{\widetilde{t}_R} = m^2_{\widetilde{U}_3} + m_Z^2 \cos 2\beta \hat{s}^2 Q_u + m_t^2, \tag{4.3c}$$

where $\hat{s}^2 = \sin^2\theta_W(m_Z)_{\overline{\rm MS}}$. The diagonal elements of the mass-squared matrices for the other sfermions are obtained by replacing $(m_{\widetilde{Q}_3}, m_{\widetilde{U}_3})$ by $(m_{\widetilde{Q}_3}, m_{\widetilde{D}_3})$ for $\widetilde{b}$, $(m_{\widetilde{Q}}, m_{\widetilde{U}})$ for $\widetilde{u}$, $(m_{\widetilde{Q}}, m_{\widetilde{D}})$ for $\widetilde{d}$, $(m_{\widetilde{L}_3}, m_{\widetilde{E}_3})$ for $\widetilde{\tau}$, $(m_{\widetilde{L}}, m_{\widetilde{E}})$ for $\widetilde{e}$, and by choosing appropriate values for the third component of the weak isospin I_{3f} and the electric charge Q_f. The off-diagonal elements in (4.3a), $m_t A^t_{\rm eff}$, should be replaced by $m_f A^f_{\rm eff}$

$$A^f_{\rm eff} = \begin{cases} A_f - \mu^* \cot\beta & (f = t) \\ A_f - \mu^* \tan\beta & (f = b, \tau) \end{cases} \tag{4.4}$$

for $\widetilde{b}$ and $\widetilde{\tau}$, while it is set to zero for the other sfermions. The sfermion mass-squared matrix can be diagonalized by using the unitary matrix $U^{\widetilde{f}}$ for $\widetilde{f} = \widetilde{t}, \widetilde{b}, \widetilde{\tau}$:

$$(U^{\widetilde{f}})^\dagger M^2_{\widetilde{f}} U^{\widetilde{f}} = {\rm diag}(m^2_{\widetilde{f}_1}, m^2_{\widetilde{f}_2}), \qquad (m_{\widetilde{f}_1} < m_{\widetilde{f}_2}). \tag{4.5}$$

In all our numerical examples, we put real values for A_f and μ. Since we neglect the left-right mixing in the first two generations, their mass eigenvalues are given by the diagonal elements.

It is useful to examine analytic expressions of the S and T parameters under some approximations. If the mixing between the left- and right-handed states is negligible, the sfermion contribution to the S parameter, ΔS, can be given by the following simple form:

$$\Delta S = -\frac{1}{\pi m_Z^2} \sum_f C_f I_{3f} Y_{f_L} F_5(m_Z^2 : m_{\widetilde{f}_L}, m_{\widetilde{f}_L}), \tag{4.6}$$

where C_f is 3 for the squarks and 1 for the sleptons. The symbol f runs over the flavor space. In this limit, only the $\mathrm{SU}(2)_L$ doublets contributes to the S parameter. The explicit form of the function $F_5(m_Z^2 : m_{\widetilde{f}}, m_{\widetilde{f}})$ in the first line has been given in ref. [23]. Since ΔS is proportional to the hypercharge Y_f, the relative sign of ΔS is opposite between squarks ($Y_q = 1/6$) and sleptons ($Y_L = -1/2$) in the first two generations. Moreover, since ΔS is proportional to I_{3f}, it receives contribution only when there is a mass splitting among $\mathrm{SU}(2)_L$ multiplet members. It takes a particularly simple form in the large sfermion mass limit. For example, the $\widetilde{u}_L$-$\widetilde{d}_L$ and $\widetilde{\nu}_l$-$\widetilde{l}_L$ contributions can be expressed as

$$(\Delta S)_{\widetilde{q}} \approx -\frac{1}{12\pi} \frac{m^2_{\widetilde{u}_L} - m^2_{\widetilde{d}_L}}{m^2_{\widetilde{u}_L} + m^2_{\widetilde{d}_L}} \left[1 + O\left(\frac{m^2_{\widetilde{u}_L} - m^2_{\widetilde{d}_L}}{m^2_{\widetilde{u}_L} + m^2_{\widetilde{d}_L}}\right)\right], \tag{4.7a}$$

$$(\Delta S)_{\widetilde{l}} \approx +\frac{1}{12\pi} \frac{m^2_{\widetilde{\nu}_l} - m^2_{\widetilde{l}_L}}{m^2_{\widetilde{\nu}_l} + m^2_{\widetilde{l}_L}} \left[1 + O\left(\frac{m^2_{\widetilde{\nu}_l} - m^2_{\widetilde{l}_L}}{m^2_{\widetilde{\nu}_l} + m^2_{\widetilde{l}_L}}\right)\right], \tag{4.7b}$$

respectively. The magnitude of ΔS is determined by the mass difference between the up- and down-type states in the SU$(2)_L$ doublet. Except for the $\widetilde{t}_L$-$\widetilde{b}_L$ case, the mass difference of the up- and down-type components of the SU(2) doublets is determined by the D-terms in the mass-squared matrix by neglecting the tiny contribution from the fermion masses

$$m^2_{\widetilde{\nu}_l} - m^2_{\widetilde{l}_L} = m^2_{\widetilde{u}_L} - m^2_{\widetilde{d}_L} = (1-\hat{s}^2)m_Z^2\cos 2\beta. \tag{4.8}$$

Since the r.h.s. of eq. (4.8) is negative for $\tan\beta > 1$ and its magnitude grows as $\tan\beta$ increases, we can understand the qualitative behavior of the squark and slepton contributions in Fig. 3.

The analytic form of the T parameter in the zero left-right mixing limit of squarks and sleptons are also simple. It also receives contribution from particles which carry the SU$(2)_L$ quantum number. For example, the $\widetilde{t}_L$-$\widetilde{b}_L$ contribution is given by

$$\begin{aligned}\Delta T &= \frac{G_F}{\sqrt{2}}\frac{1}{4\pi^2\alpha}C_f\Big[\frac{1}{2}(m^2_{\widetilde{t}_L}+m^2_{\widetilde{b}_L}) + \frac{m^2_{\widetilde{t}_L}m^2_{\widetilde{b}_L}}{m^2_{\widetilde{t}_L}-m^2_{\widetilde{b}_L}}\ln\frac{m^2_{\widetilde{b}_L}}{m^2_{\widetilde{t}_L}}\Big]\\ &\approx \frac{G_F}{24\sqrt{2}\pi^2\alpha}C_f\frac{(m^2_{\widetilde{t}_L}-m^2_{\widetilde{b}_L})^2}{m^2_{\widetilde{t}_L}+m^2_{\widetilde{b}_L}}\Big[1+O\Big(\frac{m^2_{\widetilde{t}_L}-m^2_{\widetilde{b}_L}}{m^2_{\widetilde{t}_L}+m^2_{\widetilde{b}_L}}\Big)\Big].\end{aligned} \tag{4.9}$$

The second line in eq. (4.9) is an expression in the large $\widetilde{t}_L$, $\widetilde{b}_L$ mass limit. Contributions from the other squarks and sleptons are obtained by replacing the masses and C_f factors appropriately. The squarks in the first two generations and sleptons contributions can be found by replacing the mass parameters and C_f appropriately. Since the function in the parenthesis of eq. (4.9) is positive for any values of $(m_{\widetilde{u}_L}, m_{\widetilde{d}_L})$ or $(m_{\widetilde{\nu}_l}, m_{\widetilde{l}_L})$, ΔT always receives positive contributions from the squarks and sleptons.

The special attention should be payed for the stop-sbottom contribution. There is a large mass difference between $\widetilde{t}_L$ and $\widetilde{b}_L$, which is dominated by $m_t^2 - m_b^2$. It is rather easy to understand that the effect of the left-right mixing of the stop and sbottom qualitatively. Since the off-diagonal elements of the mass-squared matrices of the stop and sbottom are multiplied by the top and bottom mass squared, respectively, the effect of the left-right mixing in the stop sector is much larger than that in the sbottom sector. Let us focus on the left-right mixing in the stop mass matrix for brevity. Suppose that only $\widetilde{t}_1$ is light and the other squarks are heavy and degenerate. Suppose also that there is no mixing between $\widetilde{b}_L$ and $\widetilde{b}_R$. With these assumptions, the squark contribution to ΔT in the third generation may be parametrized by $m_{\widetilde{t}_1}$ and $m_{\widetilde{b}_L}$ ($\approx m_{\widetilde{t}_2} \approx m_{\widetilde{b}_R}$) and the unitary matrix $U^{\widetilde{t}}$. Then, the stop-sbottom contribution to ΔT is give by

$$\Delta T \approx \frac{G_F}{\sqrt{2}}\frac{1}{4\pi^2\alpha}C_q\Big[|U^{\widetilde{t}}_{11}|^2 F_5(0:m_{\widetilde{t}_1}, m_{\widetilde{b}_L}) - |U^{\widetilde{t}}_{11}|^2|U^{\widetilde{t}}_{21}|^2 F_5(0:m_{\widetilde{t}_1}, m_{\widetilde{b}_L})\Big]$$

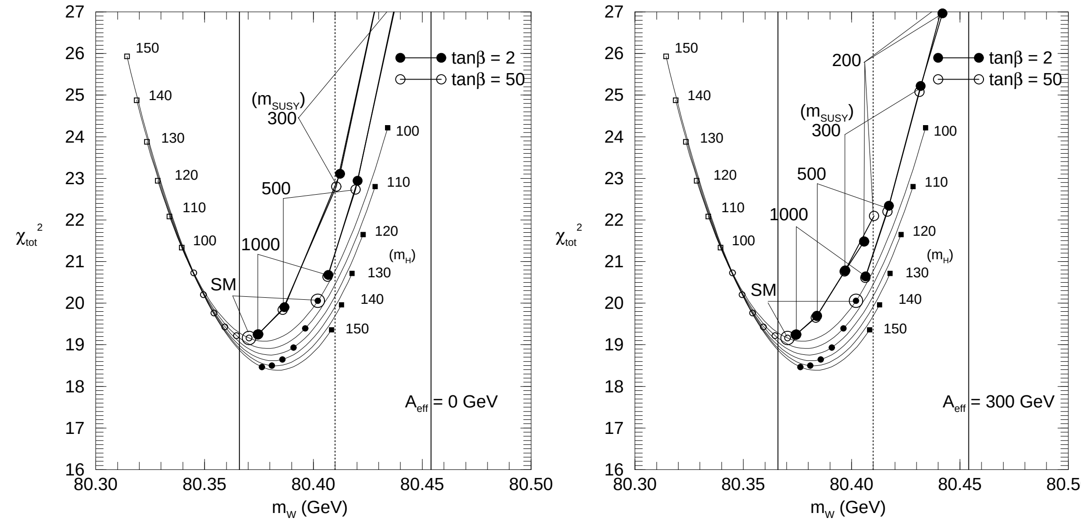

Figure 4: The squark and slepton contributions to m_W for $\tan\beta = 2$ and 50. The SUSY breaking scalar masses for the left- and right-handed squarks/sleptons are taken to be common, which are denoted by $m_{\rm SUSY}$. Two cases of the left-right mixing, $A_{\rm eff} = 0$ GeV (left) and $A_{\rm eff} = 300$ GeV (right) are examined. In each figure, two cases of the SM reference point, $(m_t({\rm GeV}), m_{H_{\rm SM}}({\rm GeV})) = (175, 100)$ and $(170, 100)$, are marked by circles.

$$\approx \frac{G_F}{\sqrt{2}} \frac{1}{4\pi^2\alpha} C_q |U_{11}^{\tilde{t}}|^4 F_5(0 : m_{\tilde{t}_1}, m_{\tilde{b}_L})$$

$$\approx \frac{G_F}{\sqrt{2}} \frac{1}{4\pi^2\alpha} C_q |U_{11}^{\tilde{t}}|^4 \Big[\frac{1}{2}(m_{\tilde{t}_1}^2 + m_{\tilde{b}_L}^2) + \frac{m_{\tilde{t}_1}^2 m_{\tilde{b}_L}^2}{m_{\tilde{t}_1}^2 - m_{\tilde{b}_L}^2} \ln \frac{m_{\tilde{b}_L}^2}{m_{\tilde{t}_1}^2} \Big]. \tag{4.10}$$

Let us recall that the left-right mixing is induced by $A_{\rm eff}^t$ in eq. (4.4). The factor $|U_{11}^{\tilde{t}}|^4$ decreases (≤ 1) as $A_{\rm eff}^t$ increases and it suppresses ΔT. The behavior of the squark contribution in Fig. 3 may be interpreted in this way. On the other hand, if only $m_{\tilde{t}_1}$ is kept small in eq. (4.10) while keeping $|U_{11}^{\tilde{t}}|$ finite, the T parameter grows with $m_{\tilde{b}_L}^2$. This reflects the growth of the $A_{\rm eff}^t$ parameter as $(m_{\tilde{b}_L}^2/m_t)|U_{11}^{\tilde{t}}|^2/(1 - |U_{11}^{\tilde{t}}|^2)$, that breaks the custodial SU(2) symmetry [26].

Let us give the analytic expression of ΔR in the large sfermion mass limit. Because ΔR is a linear combination of the Z-boson propagator corrections between two different momentum transfer scales, there are contributions not only from the left-handed sfermions but also from the right-handed sfermions. By taking $m_{\tilde{f}_L}$ and $m_{\tilde{f}_R}$ as the left- and right-handed sfermion masses, respectively, ΔR in the heavy mass limit is given by

$$\Delta R \approx -\frac{1}{30\pi} C_f \Big[(I_{3f} - \hat{s}^2 Q_f)^2 \frac{m_Z^2}{m_{\tilde{f}_L}^2} + (\hat{s}^2 Q_f)^2 \frac{m_Z^2}{m_{\tilde{f}_R}^2} \Big]. \tag{4.11}$$

Although the negative sign of ΔR leads to negative contribution to ΔT_Z in (2.12b), its magnitude is so tiny that the net contribution of sfermions to ΔT_Z is found to be always positive.

In Fig. 4, we superimposed the sfermion contribution to m_W and to the total χ^2. $A_{\rm eff} = 0$ and $A_{\rm eff} = 300$ GeV cases are shown side by side. Because the total χ^2 is not a linear sum of the SM contribution and the new physics contribution, we show two representative cases of the reference SM point, one for $(m_t, m_{H_{\rm SM}}) = (175, 100)$ and the other for $(m_t, m_{H_{\rm SM}}) = (170, 100)$ in GeV units. For each representative $(m_t, m_{H_{\rm SM}})$ case, we show the MSSM predictions of m_W and the total χ^2 as a function of the common sfermion mass $m_{\rm SUSY}$. Here, for simplicity, we set all the 10 sfermion mass parameters in eqs. (3.1d) and (3.1e) to have a common value $m_{\rm SUSY}$, and the 3 $A^f_{\rm eff}$ parameters in eq. (4.4) to have a common value $A_{\rm eff}$. We find that the sfermion contributions always make m_W larger than the SM prediction. Because the SM prediction for m_W is smaller than the experimental mean value at $m_t \lesssim 170$ GeV, the sfermion contribution can improve the fit for m_W. As may be seen from the four examples in Fig. 4, however, the sfermion contribution always make the overall fit worse than the SM. By comparing the $A_{\rm eff} = 0$ case (left) and the $A_{\rm eff} = 300$ GeV case (right), we find that the unfavorable sfermion contribution can be made small by introducing $A_{\rm eff}$ for the same value of $m_{\rm SUSY}$. The trend can be understood qualitatively by using the analytic expressions (4.7), (4.9) and (4.10) for the sfermion contributions to the S and T parameters. The sfermion contribution to the U parameter is found numerically small.

As is clear from the figures, the present m_W data gives little contribution to the total χ^2 of the fit. Although the positive contribution to Δm_W can improve the fit to the m_W data if $m_t \sim 170$ GeV, the overall χ^2 always gets worse because of the Z-parameter constraints as summarized in Fig. 3.

4.2 MSSM Higgs bosons

The MSSM has an extended Higgs boson sector with three neutral Higgs bosons, h, H, and A, and one charged Higgs boson $H^{\pm}$. All their masses and couplings are calculated in terms of the MSSM Lagrangian parameters, by using the improved one-loop potential [12]. Their contribution to the oblique parameters are evaluated carefully, because parts of the SM corrections contain the $m_{H_{\rm SM}}$ dependence from the two-loop corrections. They appear in the T parameter and in the Δg^b_L parameter, although the $m_{H_{\rm SM}}$ dependence of the latter turned out to be negligibly small. In order to avoid discontinuity in the theoretical predictions because of the lack of the corresponding two-loop results in the MSSM, we make the following arrangement in our actual calculation. For each MSSM parameters, we first calculate the lightest CP-even neutral Higgs boson mass, m_h. We then evaluate all the SM corrections for $m_{H_{\rm SM}} = m_h$. The contributions of the MSSM Higgs sector to the radiative corrections are then evaluated as the sum of the SM contributions, that partially contain the two-loop correction, and the difference between the MSSM and the SM Higgs sector contributions that is calculated strictly in the one-loop order by using the formulae in the Appendices. In this way, we can test numerically the decoupling of the MSSM Higgs sector in the large m_A limit.

In Fig. 5, we show the contributions of the MSSM Higgs sector to the ΔS_Z and ΔT_Z parameters when $m_A = 50$ GeV, 100 GeV and 300 GeV. As always, the results for $\tan\beta = 2$ are shown by solid blobs, and those for $\tan\beta = 50$ are shown by open blobs. We find that the MSSM prediction is remarkably near to the SM prediction at $m_{H_{\rm SM}} = m_h$ already at $m_A = 300$ GeV. The lightest Higgs boson mass in ref.[12] can be approximately expressed as

$$m_h \approx 102 - 6.7 \ln \frac{\tan\beta}{2} + \frac{\tan\beta - 2}{\tan\beta}(0.13 \tan\beta + 43.5)$$

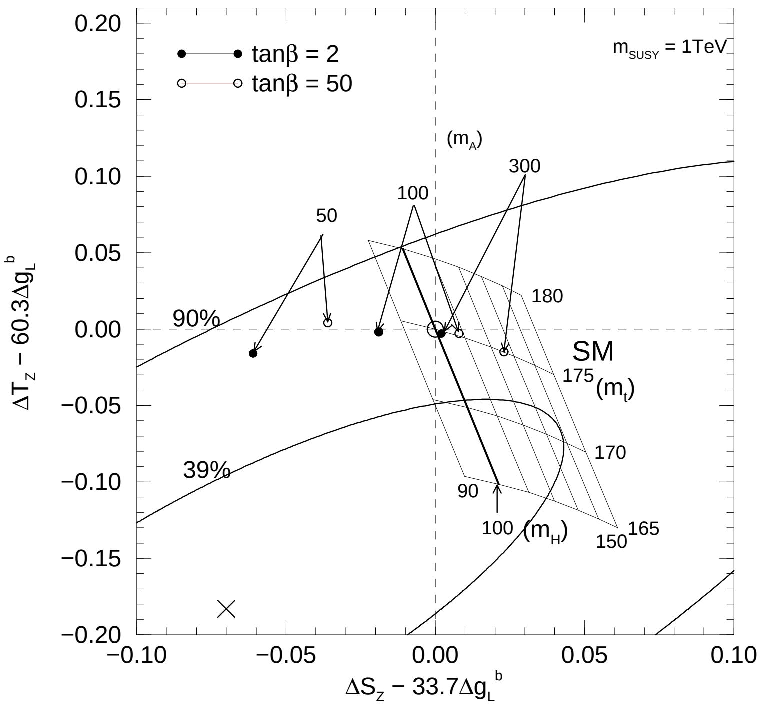

Figure 5: Contributions to $(\Delta S_Z, \Delta T_Z)$ from the Higgs bosons for $\tan\beta = 2$ and 50. The 1-loop improved Higgs potential, in which only the top and bottom Yukawa couplings are retained, are used to find the mass eigenvalues. The inputs are the pseudo-scalar Higgs-boson mass m_A and $\tan\beta$. Three values of m_A, $m_A = 50, 100$ and 300 GeV are examined. The scale parameter $m_{\rm SUSY}$ which appears in the 1-loop potential is set at 1 TeV.

$\tan\beta$	m_A	m_h	m_H	m_{H^-}	ΔS_Z	ΔT_Z	Δm_W	$\chi^2_{\rm tot}$
2	50	49.1	137	94.7	−0.061	−0.016	0.021	23.2
	100	75.0	152	128	−0.019	−0.002	0.007	21.0
	200	97.3	222	216	−0.003	−0.003	0.000	20.0
	300	102	313	311	0.002	−0.003	−0.002	19.8
	1000	106	1004	1003	0.006	−0.003	−0.003	19.7
50	50	50.3	129	94.7	−0.036	0.004	0.023	22.7
	100	100	129	128	0.008	−0.003	−0.003	19.6
	200	128	200	216	0.020	−0.014	−0.012	18.8
	300	129	300	311	0.023	−0.015	−0.014	18.7
	1000	129	1000	1003	0.025	−0.017	−0.015	18.7

Table 3: Oblique parameters, $\Delta S_Z, \Delta T_Z$ and Δm_W in the MSSM Higgs sector for $\tan\beta = 2$ and 50. The mass spectrum of the Higgs bosons are calculated by using the 1-loop improved scalar potential which is approximated by retaining only the top- and bottom-quark Yukawa couplings [12]. The scale parameter $m_{\rm SUSY}$ which appears in the 1-loop potential is set at 1 TeV.

$$+20x_{\rm SUSY}\Big[1-0.08x_{\rm SUSY}\Big\{1+1.5\Big(1-\frac{2}{\tan\beta}\Big)\Big\}\Big], \tag{4.12}$$

when $m_A = 300$ GeV. The parameter $x_{\rm SUSY}$ is defined by $x_{\rm SUSY} \equiv \ln(m_{\rm SUSY}/1\ \text{TeV})$. Eq. (4.12) is valid for $2 \le \tan\beta \le 50$ and 1 TeV $\le m_{\rm SUSY} \le$ 2 TeV in which the error is smaller than 0.6 GeV.

We find $m_h = 102$ GeV and 129 GeV for $\tan\beta = 2$ and 50, respectively, at $m_A = 300$ GeV for $m_{\rm SUSY} = 1$ TeV, and the predictions are remarkably near to the SM predictions at $m_{H_{\rm SM}} = m_h$. The m_A dependence of the MSSM predictions are shown in Table 3, together with the masses of all the MSSM Higgs bosons for $\tan\beta = 2$ and 50 and at $m_{\rm SUSY} = 1$ TeV. From the Table, we can see that the predictions of the MSSM reduces essentially to those of the SM at $m_{H_{\rm SM}} = m_h$ when $m_A \gtrsim 200$ GeV.

4.3 Supersymmetric fermions: charginos and neutralinos

In this subsection, we study the contributions of the charginos and neutralinos. The chargino and neutralino mass matrices depend on four parameters, the two gaugino masses M_1 and M_2, the supersymmetric Higgs-mixing mass μ and $\tan\beta$. Because the gaugino masses and the Higgs-mixing mass are invariant under the electroweak gauge symmetry, they contribute neither to the S nor the T parameter.

On the other hand, because they are fermions, their virtual creation can affect the running of the gauge-boson propagator, the R parameter (2.9), strongly when the pair-creation threshold is near the Z-boson pole [23, 39].

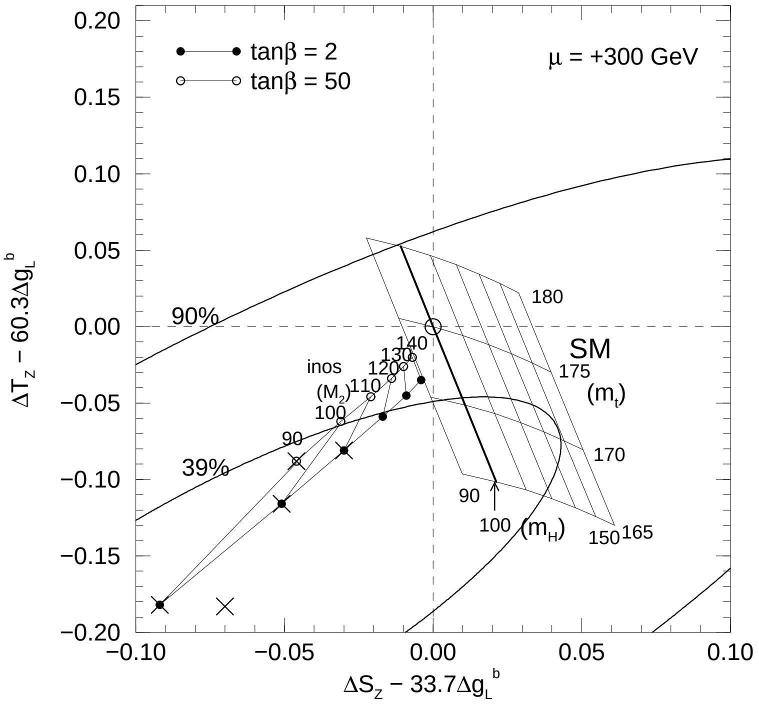

Figure 6: The chargino and neutralino contributions to $(\Delta S_Z, \Delta T_Z)$ for $\tan\beta = 2$ and 50. The supersymmetric Higgs-mixing mass μ is fixed at $\mu = 300$ GeV. The GUT relation for the gaugino masses, $M_2/\hat{\alpha}_2 = M_1/\hat{\alpha}_1$ is assumed, and cases for $M_2 = 140 \sim 90$ GeV are shown by using the marked SM reference point at $(m_t, m_{H_{\rm SM}}) = (175, 100)$ in GeV unit as the origin. Those points with the cross $(\times)$ symbols give the lighter chargino mass $m_{\tilde{\chi}_1^-}$ below 90 GeV.

Although the present lower mass bound on the charginos is as large as the Z-boson mass rather than its half, we find that the effect can still be significant. We show in Fig. 6 the contributions of the charginos and neutralinos to the ΔS_Z and ΔT_Z parameters. In the figure, the supersymmetric Higgs mass is fixed at $\mu = 300$ GeV, and the SU(2)$_L$ gaugino mass M_2 has been varied. The U(1)$_Y$ gaugino mass is scaled by the relation $M_1/M_2 = \hat{\alpha}_1/\hat{\alpha}_2$ for definiteness. The case for $\tan\beta = 2$ are shown by solid blobs, and those for $\tan\beta = 50$ are shown by open blobs. As the M_2 decreases, the lightest chargino mass decreases, and those points with the cross symbol give the chargino mass below the direct search bound (3.5).

Most importantly, we find that the effect of relatively light charginos and neutralinos gives *both* ΔS_Z *and* ΔT_Z negative, which improves the fit over the SM. This is essentially because of the R parameter that reside both in the ΔS_Z and the ΔT_Z parameters (2.12). For instance, if the wino-like chargino mass is near to

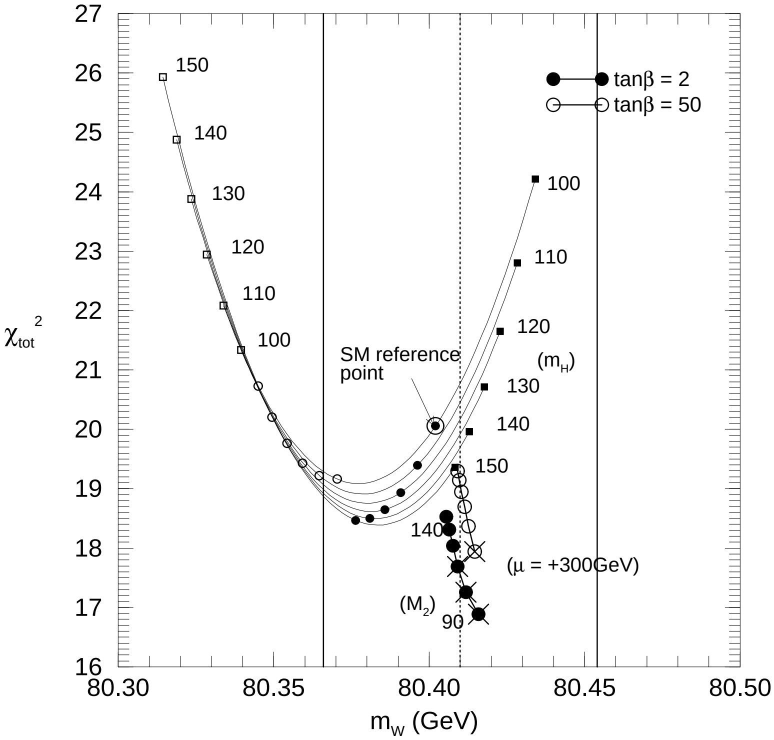

Figure 7: The chargino and neutralino contributions to $(m_W, \chi^2_{\rm tot})$ for $\tan\beta = 2$ and 50. The supersymmetric Higgs-mixing mass μ is fixed by $\mu = 300$ GeV. The GUT relation for the gaugino masses, $M_2/\hat{\alpha}_2 = M_1/\hat{\alpha}_1$ is assumed. The 6 blobs are for $M_2({\rm GeV}) = 140, 130, 120, 110, 100, 90$ at $\tan\beta = 2$ (solid blobs) and at $\tan\beta = 50$ (open blobs). Those points with the cross (×) symbols indicate that the lightest chargino mass $m_{\widetilde{\chi}_1^-}$ is smaller that 90 GeV.

half the Z-boson mass, its contribution to the parameter R behaves as

$$\Delta R \approx -\hat{c}^4\Big(\frac{1}{\beta} - \frac{16}{3\pi}\Big), \tag{4.13}$$

where $\hat{c}^2$ is given by $\hat{c}^2 = 1 - \hat{s}^2$. $\beta = \sqrt{4M_2^2/m_Z^2 - 1}$ is the analytic continuation of the chargino velocity below the threshold. When $4M_2^2/m_Z^2 \gg 1$, the effect is suppressed as

$$\Delta R \approx -\frac{4\hat{c}^4}{15\pi}\frac{m_Z^2}{M_2^2}\Big[1 + O\Big(\frac{m_Z^2}{M_2^2}\Big)\Big]. \tag{4.14}$$

The chargino contribution to ΔR is negative just like the sfermion contribution to ΔR in eq. (4.11). The coefficient of the wino contribution in eq. (4.14) is found to be about 90 times larger than that of the $\widetilde{l}_R$ contribution. This large negative contribution to ΔR makes both ΔS_Z and ΔT_Z significantly negative when a relatively light chargino of mass about 100 GeV exists.

μ	M_2	$m_{\tilde{\chi}_1^-}$	$m_{\tilde{\chi}_1^0}$	ΔR	ΔS_Z	ΔT_Z	Δm_W	$\chi^2_{\rm tot}$
+300	110	85.0	45.9	−0.070	−0.030	−0.081	0.007	17.7
	120	93.8	50.9	−0.054	−0.017	−0.059	0.006	18.0
	130	103	55.9	−0.044	−0.009	−0.045	0.004	18.3
	140	111	60.8	−0.036	−0.004	−0.035	0.004	18.5
−300	70	82.2	38.1	−0.082	−0.058	−0.104	0.010	17.8
	80	91.7	43.2	−0.062	−0.041	−0.076	0.008	18.2
	90	101	48.3	−0.049	−0.030	−0.058	0.007	18.5
	100	111	53.3	−0.040	−0.023	−0.046	0.006	18.8
+105	300	80.5	62.4	−0.045	0.009	−0.057	−0.007	17.7
+115	300	89.4	69.8	−0.036	0.013	−0.043	−0.006	18.0
+127	300	100	78.7	−0.028	0.014	−0.032	−0.005	18.2
+137	300	109	85.4	−0.024	0.015	−0.026	−0.004	18.4
−68	300	80.2	64.2	−0.056	−0.041	−0.071	0.007	18.4
−78	300	89.8	73.9	−0.042	−0.029	−0.051	0.006	18.8
−89	300	101	84.7	−0.032	−0.021	−0.037	0.005	19.1
−99	300	110	94.4	−0.027	−0.016	−0.028	0.005	19.3

Table 4: Chargino and neutralino contributions to the oblique parameters, $\Delta R, \Delta S_Z, \Delta T_Z, \Delta m_W$ and the total χ^2 of the fit at $\tan\beta = 2$.

More detailed numerical results are summarized in Table 4 for $\tan\beta = 2$ and in Table 5 for $\tan\beta = 50$. From both tables, we can see that ΔT_Z is always negative for these inputs and its magnitude is dominated by ΔR, see eq. (2.12b). On the other hand, ΔS_Z and Δm_W can be positive or negative. As compared to the total χ^2 value of 20.1 which is obtained at the SM reference value $(m_t(\text{GeV}), m_{H_{\rm SM}}(\text{GeV}), \alpha(m_Z^2)) = (175, 100, 129.90)$ under the $\alpha_s(m_Z)$ constraint (2.25c), see eq. (4.1), we find an improvement of $\chi^2_{\rm tot}$ in the tables by between 1.0 and 1.9, by including the contribution of a chargino if its mass is around 100 GeV, just above the present mass bound.

4.4 Summary of oblique corrections

We show in Fig. 8 the contributions of all the sectors of the MSSM together. The total oblique corrections are obtained by summing the SM contribution for one's favorite m_t at $m_{H_{\rm SM}} = 100$ GeV, the MSSM Higgs sector contribution, the squark contribution, the slepton contribution, and the chargino-neutralino contribution vectorially in the plane.

μ	M_2	$m_{\tilde{\chi}_1^-}$	$m_{\tilde{\chi}_1^0}$	ΔR	ΔS_Z	ΔT_Z	Δm_W	$\chi^2_{\rm tot}$
$+300$	90	82.9	43.8	-0.077	-0.046	-0.089	0.013	17.9
	100	92.1	48.7	-0.059	-0.031	-0.063	0.011	18.4
	110	101	53.6	-0.047	-0.021	-0.046	0.009	18.7
	120	110	58.4	-0.039	-0.014	-0.034	0.008	18.9
-300	90	84.6	44.4	-0.074	-0.044	-0.084	0.012	18.0
	100	93.8	49.3	-0.057	-0.030	-0.060	0.011	18.4
	110	103	54.1	-0.045	-0.020	-0.044	0.009	18.8
	120	112	59.0	-0.038	-0.014	-0.033	0.008	19.0
$+87$	300	80.2	64.7	-0.049	-0.011	-0.054	0.003	18.1
$+98$	300	90.5	74.0	-0.037	-0.004	-0.036	0.003	18.5
$+108$	300	99.7	82.2	-0.030	-0.001	-0.026	0.003	18.8
$+120$	300	110	91.0	-0.025	$+0.001$	-0.018	0.004	19.1
-85	300	79.8	64.5	-0.050	-0.013	-0.056	0.003	18.1
-96	300	90.2	74.0	-0.038	-0.006	-0.037	0.004	18.5
-107	300	100	83.2	-0.030	-0.002	-0.026	0.004	18.9
-117	300	110	91.2	-0.025	$+0.000$	-0.019	0.004	19.1

Table 5: Chargino and neutralino contributions to the oblique parameters, $\Delta R, \Delta S_Z, \Delta T_Z, \Delta m_W$ and the total χ^2 of the fit at $\tan\beta = 50$.

It is surprising that each sector of the MSSM gives distinctive contributions in the ΔS_Z and ΔT_Z plane. The squark sector contributes essentially to positive T_Z direction, which is strongly disfavored by the electroweak data. The slepton sector contributes negatively to S_Z, but T_Z remains constant or slightly positive for large $\tan\beta$. This is also found to be disfavored by the data. Therefore, if only the squarks and sleptons are light, their contributions would make the fit to the electroweak data significantly worse than the SM.

On the other hand, the MSSM Higgs sector is found to give the contribution very similar to that of the SM when the lightest CP-even Higgs-boson mass m_h is taken to be the SM Higgs boson mass. Therefore, if m_h is significantly larger than the reference value of 100 GeV, either with large $\tan\beta$, or by having very heavy squark masses that affect the effective scalar potential, the fit improves slightly.

Finally, the contribution of charginos and neutralinos make both ΔS_Z and ΔT_Z negative, and hence the fit improves more significantly if the lightest chargino mass is near the present direct search limit of around 100 GeV.

As emphasized in section 2, the oblique corrections dominate the whole radiative effects if either squarks and sleptons, or the charginos and neutralinos are

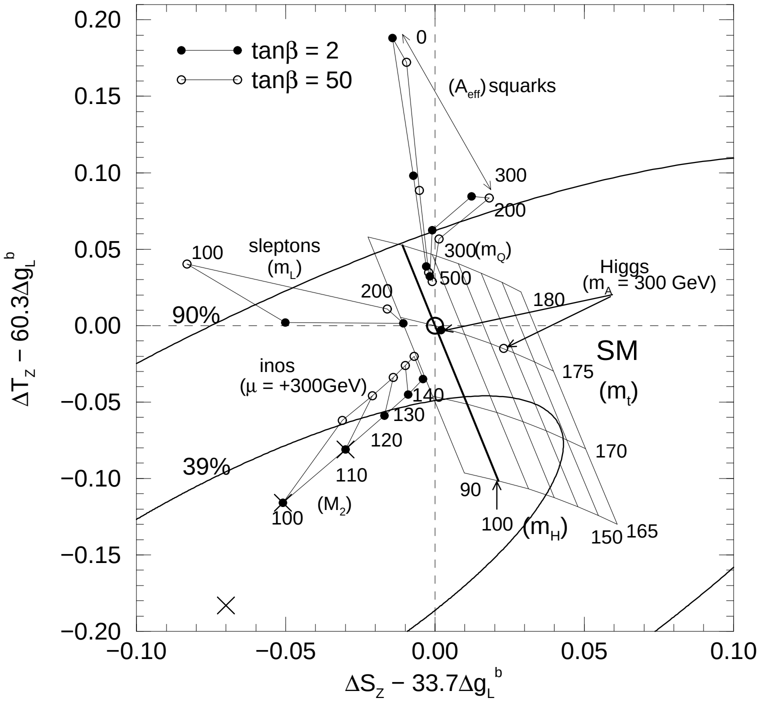

Figure 8: Summary of the supersymmetric contributions to $(\Delta S_Z, \Delta T_Z)$.

very heavy. Otherwise, in addition to the oblique corrections summarized in this Figure, there will be additional vertex and box corrections.

5 Non-oblique corrections

We found in the previous section that the existence of relatively light charginos (of mass $\sim$ 100 GeV) improves the SM fit to the electroweak data, whereas the existence of relatively light squarks and sleptons (of mass $\sim$ 100 GeV) makes the fit significantly worse. On the other hand, if both supersymmetric fermions (charginos and neutralinos) and supersymmetric scalars (squarks and sleptons) are light, then in addition to the universal gauge-boson-propagator corrections (the oblique corrections), we should expect process specific vertex and box corrections to be non-negligible. We would like to address this problem in this section.

There are just two types of process specific corrections which are relevant for the precision electroweak experiments on the Z-boson properties and the W-boson mass. One is the vertex corrections to various $Z \to f\overline{f}$ amplitudes, the parameters Δg_α^f, in eqs.(2.4). Even if we assume the universality of the first two generation squarks and sleptons, there are 14 independent Zff vertex corrections in the MSSM. The other is the vertex and box corrections to the muon-decay amplitude, the parameter $\Delta\overline{\delta}_G$, that affect the ΔT_Z parameter (2.12b) in the Z-boson experiments and the Δm_W parameter (2.20b) for the W-boson mass. Although this is just a single correction factor, it affects all the electroweak predictions because we use the observed magnitude of the muon decay constant G_F as one of the basic inputs of our calculation.

We present our studies on these non-oblique corrections step by step in the increasing order of the number of observables that will be affected. In section 5.1 we study the MSSM Higgs boson contribution to the Zbb, $Z\tau\tau$ and $Z\nu_\tau\nu_\tau$ vertices. In section 5.2, we study the order α_s vertex correction when gluinos and squarks are both light. This will affect the Zqq vertices only, and we find it useful to study its quantitative significance independently of the other electroweak corrections. In section 5.3, we study the electroweak corrections to the Zqq vertices when both squarks and charginos/neutralinos are light. Effects on the Zbb vertices are carefully studied. In section 5.4, we study the Zll vertices when both sleptons and charginos/neutralinos are light. We notice, however, if both the supersymmetric fermions (charginos and neutralinos) and the sleptons are light enough to affect the Zll vertices significantly, they should also affect the muon-decay amplitude, $\Delta\overline{\delta}_G$, and hence all the remaining electroweak observables. All the numerical results in the following subsections are found at $(m_t(\text{GeV}), \alpha_s(m_Z), \alpha(m_Z^2)) = (175, 0.118, 128.90)$.

5.1 Zff-vertex corrections by the MSSM Higgs bosons

When $\tan\beta$ is very large, the Yukawa couplings of the b-quark and the τ-lepton get large, and we expect significant vertex corrections for both Zbb and $Z\tau\tau$ vertices. The most significant contributions are found to arise from the vertices with the Higgs bosons. In Fig. 9, we show R_b, Γ_τ and the total χ^2 as functions of m_A, the pseudo-scalar Higgs-boson mass in our Higgs potential. The $\tan\beta = 2$ case is given by the solid lines, whereas the $\tan\beta = 50$ case is given by the dashed lines. For simplicity, we set all squarks and slepton masses as well as the lightest chargino mass to be 1 TeV so that their contribution can be neglected.

We find that for sufficiently small m_A at large $\tan\beta$, there is a significant positive contribution to both Γ_b and Γ_τ. These effects have been noted [40] when the experimental data on R_b larger than the SM prediction was reported [41]. We find that the fit to the latest R_b data is slightly better with larger R_b predicted in the MSSM with $\tan\beta = 50$ and $m_A \sim 60$ GeV, but as we can see from the total χ^2 behavior, the scenario is not favored over the SM. This is because the MSSM predicts light Higgs particles whose contributions to the oblique parameters worsen the fit, as shown in Table 3 in Section 4. Also the pseudo-scalar Higgs-boson mass m_A significantly below 100 GeV is not acceptable because it gives the lightest

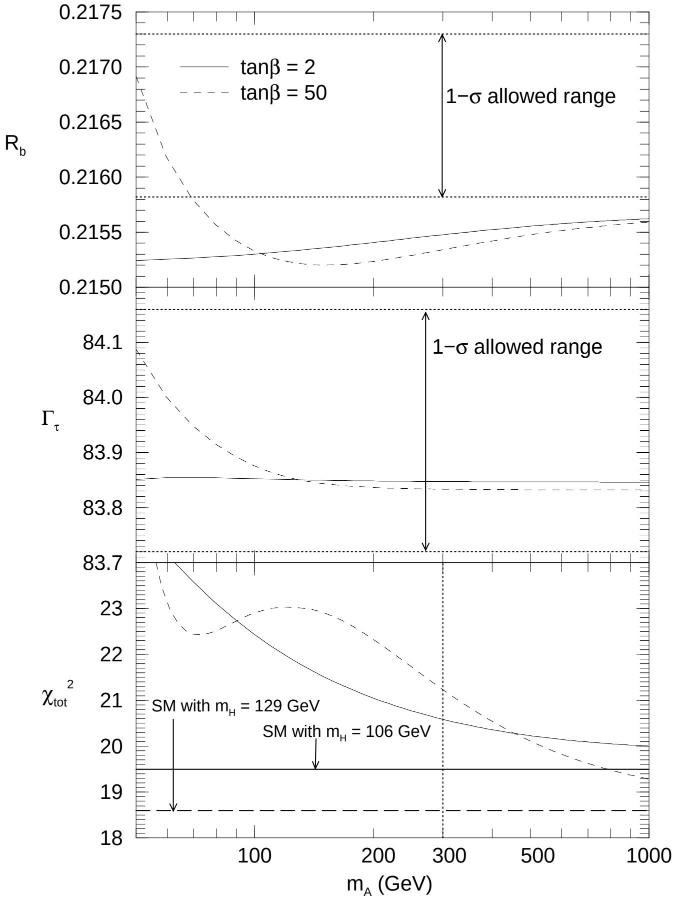

Figure 9: The Higgs boson contributions to R_b (top), Γ_τ (middle) and the total χ^2 (bottom) as functions of m_A for $\tan\beta = 2$ (solid line) and 50 (dashed line). The squarks, sleptons and lighter chargino masses are fixed by 1 TeV. The other parameters, $m_t, \alpha_s(m_Z)$ and $\alpha(m_Z^2)$ are fixed by 175 GeV, 0.118 and 128.90, respectively. The 1-σ allowed range of R_b and Γ_τ (83.94 ± 0.22 MeV [11]) are shown in the top and middle graphs, respectively. Two thick lines in the bottom graph denote the SM fit for $m_{H_{\rm SM}} =$ 106 GeV(solid) and $m_{H_{\rm SM}} = 129$ GeV(dashed) which are the lightest Higgs boson mass in the MSSM at $m_A = 1$ TeV for $\tan\beta = 2$ and 50, respectively.

CP-even Higgs boson mass (m_h) below the direct search bound (3.6).

In Fig. 9 we show by horizontal lines the $\chi^2_{\rm tot}$ of the SM prediction at $m_t =$ 175 GeV and $1/\alpha(m_Z^2) = 128.90$ for $m_{H_{\rm SM}} = 106$ GeV and 129 GeV. These Higgs boson masses correspond to the masses of the lightest CP-even Higgs boson (h) in the MSSM at $\tan\beta = 2$ and 50, respectively. Table 3 shows that the oblique corrections from the MSSM Higgs sector reduces to the SM predictions at the corresponding Higgs boson mass, $m_{H_{\rm SM}} = m_h$, already at $m_A = 300$ GeV. In contrast, Fig. 9 shows that the vertex corrections can affect the total χ^2 significantly

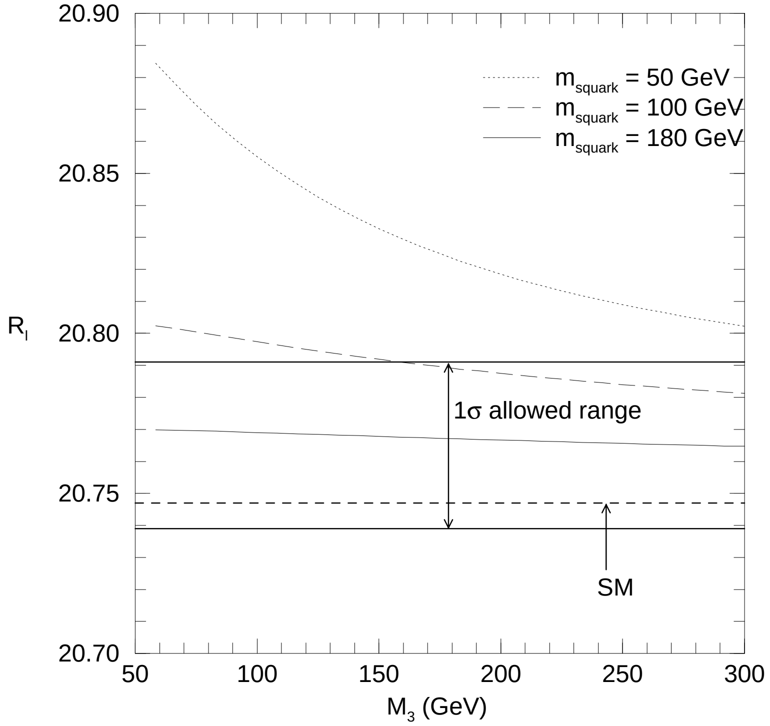

Figure 10: The SUSY-QCD correction to R_ℓ as a function of the gluino mass $M_3 = M_{\widetilde{g}}$. All the squark masses are assumed to be given by the universal scalar mass, $m_{\rm squark}$.

even at $m_A = 300$ GeV, especially for $\tan\beta = 50$. This is mainly because of the enhanced bbH and $\tau\tau H$ couplings at large $\tan\beta$, where H is the heavier of the CP-even Higgs bosons with mass $m_H \approx m_A$.

5.2 SUSY-QCD corrections

Supersymmetric QCD corrections to the Z-boson hadronic width, Γ_h, or its ratio R_ℓ to the leptonic width Γ_ℓ is one of the first vertex corrections to the Z-boson decay amplitudes calculated [8]. They contribute at the order α_s level, and hence could be significant if both squarks and gluinos are light. We would like to first examine their quantitative significance in view of the present lower mass bounds on squarks and gluinos (3.3).

The one-loop Zff amplitudes of Appendix C, which is presented by using a generic notation that apply for all the vertices and for all the MSSM corrections, take a particularly simple form when only the order α_s corrections are considered. For instance, if the mixing between the left and right chirality squarks is negligible, which we assume to be the case for the first two family squarks and sleptons, we

	Inputs (GeV)			$O(\alpha_s)$ vertex		vertex + obl.	
	$m_{\tilde{u}_L}$	$m_{\tilde{u}_R}$	$M_{\tilde{g}}$	$R_\ell/R_\ell(\mathrm{SM})$	χ^2_{SQCD}	$R_\ell/R_\ell(\mathrm{SM})$	χ^2_{tot}
I	100	100	100	1.00152	24.1	1.00241	129.1
II	180	180	180	1.00048	20.5	1.00095	52.9
III	1000	180	180	1.00003	19.9	1.00005	20.5
IV	1000	180	421	1.00001	19.8	1.00004	20.4

Table 6: The SUSY-QCD corrections to $R_\ell/R_\ell(\mathrm{SM})$ and χ^2 for $\tan\beta = 2$. In all cases, $m_{\tilde{u}_R} = m_{\tilde{d}_R}$ is assumed. The universality of the SUSY breaking scalar masses among the different generations, $m_{\tilde{Q}} = m_{\tilde{Q}_3}$, $m_{\tilde{U}} = m_{\tilde{U}_3}$ and $m_{\tilde{D}} = m_{\tilde{D}_3}$ is also assumed. The left-right mixings in the stop and sbottom sector are taken to be zero by using an appropriate values of A_t, A_b and μ. The effects of the SUSY-QCD vertex correction for four cases are summarized in the second column while the SUSY-QCD vertex correction and the oblique correction by squarks are given in the last column. Only in IV, the GUT relation $M_{\tilde{g}} = M_3 = (\hat{\alpha}_3/\hat{\alpha}_2)M_2$ has been respected. The value of $M_{\tilde{g}}$ in IV leads to $M_2 = 120$ GeV, and $m_{\tilde{\chi}_1^-} = 94$ GeV for $\mu = 300$ GeV.

find

$$\Delta g^q_\alpha = \frac{g^{qqZ}_\alpha \alpha_s}{\sqrt{4\sqrt{2}G_F m_Z^2}} \frac{32\pi}{3}\left[\Big(B_0 + B_1\Big)(0 : m_{\tilde{q}_\alpha}, M_{\tilde{g}}) \right.$$
$$\left. - 2C_{24}(m_Z^2 : m_{\tilde{q}_\alpha}, M_{\tilde{g}}, m_{\tilde{q}_\alpha})\right], \qquad (5.1)$$

where the two- and three-point functions, B_0, B_1 and C_{24} are given in ref. [23]. We reproduced the results of refs. [8].

In Fig. 10 we show the SUSY-QCD correction to the ratio R_ℓ as functions of the gluino mass $M_3 = M_{\tilde{g}}$ when all the squark masses are taken to be the same for brevity. Significantly larger magnitude of R_ℓ as compared to the SM prediction at the same α_s is found only when the common squark mass is as light as 50 GeV and the gluino is lighter than 100 GeV, consistent with the early observation [8]. Once we take into account the present lower mass bound of squarks and gluinos (3.3), the quantitative significance of the SUSY-QCD correction diminishes.

We show in Table 6 the magnitude of the SUSY-QCD correction to R_ℓ for several squark and gluino mass inputs. We should compare the percentage corrections with the present experimental accuracy of R_ℓ, which is 0.125% from Table 1. Only when all the squarks and gluino masses are around 100 GeV, we can expect non-negligible effect from this sector. When all the masses are moved up to 180 GeV, consistent with the present direct search limits (3.3), the effect on R_ℓ is about 0.05% and is already insignificant. Our studies on the oblique correction suggest that the left-handed squarks should be rather heavy not to worsen the electroweak fit. If only the right-handed squarks are kept light at 180 GeV, together with the gluino of the same mass, the effect essentially goes away, as shown for the case III in Table 6. In the last line of the Table, we study the case IV where $M_{\widetilde{g}} = M_3 = 421$ GeV, which is the mass obtained by using the 'unification' relation $M_3/M_2 = \hat{\alpha}_3/\hat{\alpha}_2$ in one of our selected MSSM points that accommodate a chargino of mass around 100 GeV. The effect diminishes to 10^{-4}.

In the following analysis, we assume that the left-handed squarks are relatively heavy ($m_{\widetilde{q}_L} \gtrsim 1$ TeV) in order not to spoil the good fit to the electroweak data. We also adopt the 'unification' relation for the three gaugino masses $M_3/\hat{\alpha}_3 = M_2/\hat{\alpha}_2 = M_1/\hat{\alpha}_1$ in all the subsequent numerical examples. Under such conditions, we find that the SUSY-QCD corrections cannot have significant effect on our electroweak studies.

5.3 Electroweak Zqq vertex corrections with squarks

In this subsection we explore the possibility that the electroweak SUSY corrections to the Zqq vertices improve the overall fit to the data. As in the case of the SUSY-QCD corrections with a gluino-squark loop, we find that $m_{\widetilde{q}_L} \approx m_{\widetilde{t}_L}$ should be kept high ($\gtrsim 1$ TeV) in order for their positive T contribution not to spoil the good overall fit of the SM.

The only case that SUSY electroweak correction to the Zqq vertices are found to give nontrivial effects is when loops of light charginos and a light $\widetilde{t}_1$ affect the Zbb vertices. We show in Fig. 11 the effect of supersymmetric vertex corrections to the ratio R_b. In order to avoid large unfavorable oblique corrections to the T parameter, we set all the $\widetilde{q}_L$ masses large by setting $m_{\widetilde{Q}} = m_{\widetilde{Q}_3} = 1$ TeV. We take the singlet squark masses at $m_{\widetilde{U}} = m_{\widetilde{U}_3} = m_{\widetilde{D}} = m_{\widetilde{D}_3} = 200$ GeV near the Tevatron search limit (3.3). The lighter stop, $\widetilde{t}_1$, can still be light enough to affect the Zb_Lb_L vertex by having large $\widetilde{t}_L$-$\widetilde{t}_R$ mixing.

In the figure we show the present 1-σ experimental bound on R_b, and the MSSM predictions as functions of the $\widetilde{t}_1$ mass. The lower part of the figure shows the total χ^2 of the fit that includes contributions from all the electroweak data in Table 1. Three cases with a light chargino ($m_{\widetilde{\chi}_1^-} \lesssim 100$ GeV) have been examined:

(i) $\widetilde{\chi}_1^-$ is almost wino $(\mu = 300 \text{ GeV}, M_2 = 120 \text{ GeV}, m_{\widetilde{\chi}_1^-} = 94 \text{ GeV})$
(ii) $\widetilde{\chi}_1^-$ is almost higgsino $(\mu = 100 \text{ GeV}, M_2 = 800 \text{ GeV}, m_{\widetilde{\chi}_1^-} = 93 \text{ GeV})$
(iii) $\widetilde{\chi}_1^-$ is almost higgsino $(\mu = 90 \text{ GeV}, M_2 = 200 \text{ GeV}, m_{\widetilde{\chi}_1^-} = 54 \text{ GeV})$

The case (iii) violates the LEP chargino mass bound (3.5). As is clear from these figures, the MSSM effects on the Zbb vertices are not significant under the present constraints on the $\widetilde{t}_1$ and $\widetilde{\chi}_1^-$ masses. The scale of the total χ^2, which is significantly below that of the SM, is set by the light chargino-neutralino contribution to the

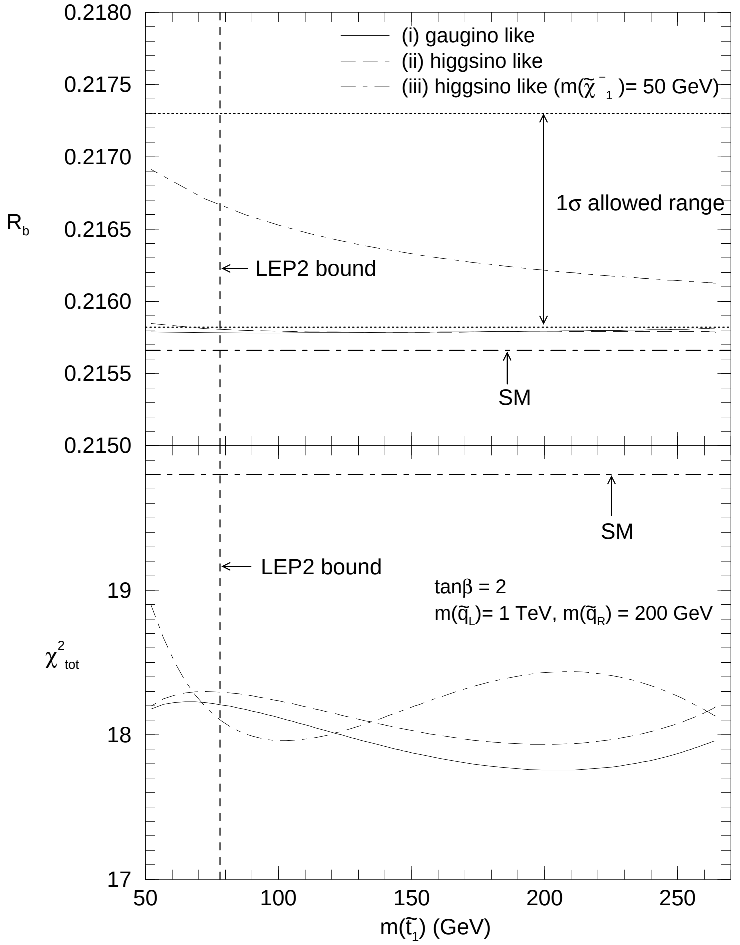

Figure 11: The stop contribution to R_b (top) and the total χ^2 (bottom) as functions of $m_{\widetilde{t}_1}$ for $m_{\widetilde{Q}} = 1$ TeV and $m_{\widetilde{U}} = m_{\widetilde{D}} = 200$ GeV where the universality in the generation space of the squark sector is assumed. Three different inputs for the chargino mass are studied: (i) $(\mu, M_2) = (300, 120)$, (ii) $(\mu, M_2) = (100, 800)$, (iii) $(\mu, M_2) = (90, 200)$ in the GeV unit. All the other SUSY particle masses are fixed by 1 TeV. The SM prediction, $R_b = 0.21566$ and $\chi^2 = 19.8$, are also shown.

oblique parameters as we explained in the last section, and the slight decrease that we observe for the cases (i) and (ii) for lighter $m_{\widetilde{t}_1}$ is not significant. Only when both the $\widetilde{t}_1$ and $\widetilde{\chi}_1^-$ are as light as 50 GeV and when the $\widetilde{\chi}_1^-$ is almost higgsino and $\widetilde{t}_1$ is almost $\widetilde{t}_R$, we could obtain significant positive contribution to R_b as discussed in the literatures a couple of years ago [9, 10]. We reproduced all the numerical results presented in ref. [10].

With the above choice of squark parameters, $m_{\widetilde{Q}} = 1$ TeV and $m_{\widetilde{U}} = m_{\widetilde{D}} = 200$ GeV, and with our neglect of all the left-right mixing in the first two generations, the electroweak vertex corrections to the four light-quark flavors are found

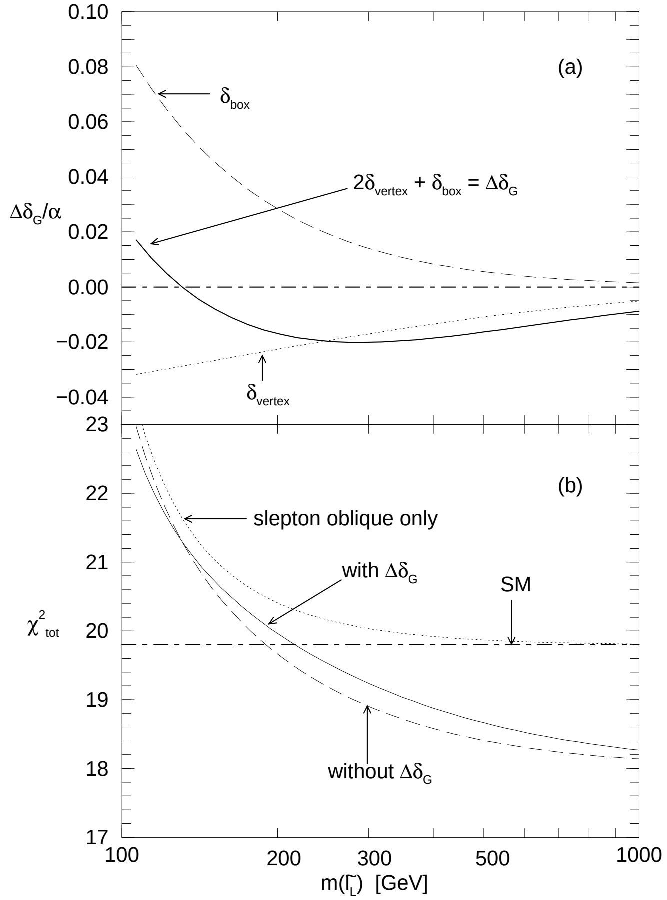

Figure 12: The MSSM contribution to $\Delta\overline{\delta}_G/\alpha$ (a) and the total χ^2 (b) as a function of the left-handed slepton mass, $m_{\tilde{l}_L}$ for $\tan\beta = 2$. In the figures, μ and M_2 are fixed at 300 GeV and 120 GeV, respectively. The GUT relation for the gaugino masses are assumed. In (a), the vertex and box corrections are shown by dotted and dashed lines, respectively. The total contribution, $2\delta_{\rm vertex} + \delta_{\rm box}$, is given by the solid line. In (b), the right-handed slepton mass is fixed by $m_{\tilde{l}_R} = 100$ GeV. The masses of squarks and Higgs bosons besides the lightest Higgs are fixed by 1 TeV. The solid and dashed lines show the total χ^2 with and without $\Delta\overline{\delta}_G$, respectively.

to be negligibly small.

5.4 Zll-vertex and μ-decay corrections with sleptons

So far, we set all the slepton masses to infinity so that they do not participate in the MSSM corrections. When sleptons are relatively light, together with relatively light charginos and neutralinos as motivated by their favorable contributions to the oblique parameters ΔS_Z and ΔT_Z, we expect two distinctive effects in the electroweak predictions of the MSSM. First, they affect the muon-decay amplitude

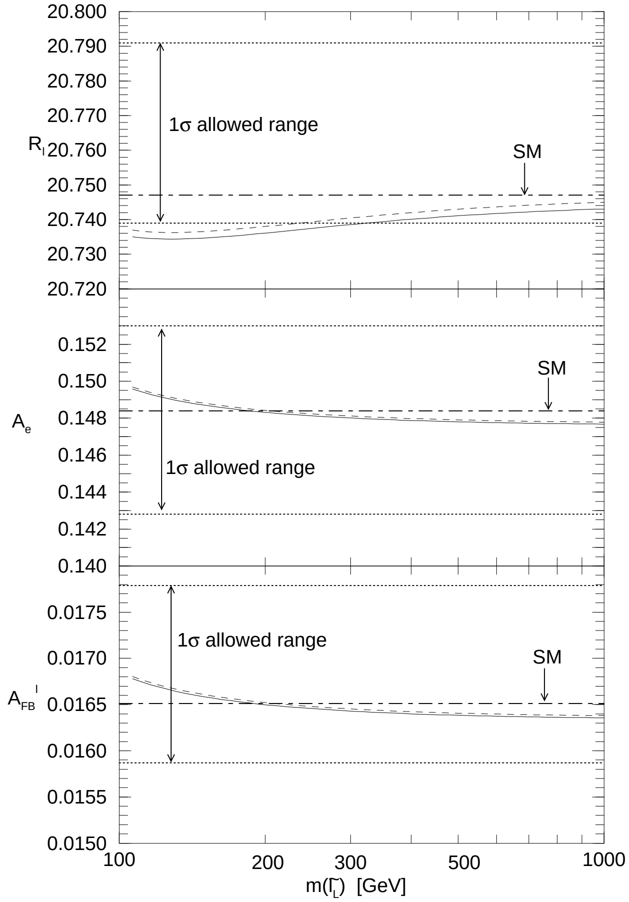

Figure 13: The scalar-lepton contributions to R_ℓ (top), A_e (middle) and $A_{\rm FB}^\ell$ (bottom) as functions of $m_{\widetilde{l}_L}$ for $\tan\beta = 2$. In each figure, the impact of the right-handed slepton mass is shown by solid ($m_{\widetilde{l}_R} = 100$ GeV) and dashed ($m_{\widetilde{l}_R} = 1$ TeV) lines, respectively. The other parameters are the same with those in Fig. 12.

and hence the parameter $\Delta\overline{\delta}_G/\alpha$, in eq. (2.10), that appear in the basic expression for the oblique parameter ΔT_Z (2.12b) and the W-boson mass (2.20b). Second, they affect the Zll vertices, and hence the parameters, $\Delta g_L^l, \Delta g_R^l, \Delta g_L^{\nu_l}$ in eqs.(2.4).

We first examine the MSSM contributions to the muon-decay amplitude carefully, because if they can make $\Delta\overline{\delta}_G/\alpha$ positive ΔT_Z can also become negative: see eq. (2.12b). A combination of this negative ΔT_Z from the muon-decay correction and the negative ΔS_Z from the oblique corrections (see Fig. 3) could improve the overall fit to the Z-pole data. If the muon-decay amplitude receives positive contribution from new physics, then it is equivalent to make the effective charged current strength larger, and the T parameter, which is a measure of the neutral-current to charged-current strengths, is effectively reduced. On the figures of the oblique parameters ΔS_Z vs. ΔT_Z, the positive $\Delta\overline{\delta}_G/\alpha$ would be regarded as the negative contribution to the ΔT_Z parameter, which is favored by the electroweak data. On the other hand, as soon as the muon-decay amplitude is affected, we should expect non-oblique Zll vertex corrections to affect the MSSM predictions for the Z-boson parameters. We therefore present in Fig. 12 the MSSM contribution to $\Delta\overline{\delta}_G/\alpha$ and that to the total χ^2, as functions of the $\tilde{l}_L$ mass by assuming $m_{\tilde{L}} = m_{\tilde{L}_3}$.

By using the analytic expressions for the muon-decay amplitude in Appendix C, we find that box corrections are always positive, while the vertex corrections are negative. After summing up, we find that the net MSSM correction to $\Delta\overline{\delta}_G$ can become positive only when $m_{\tilde{l}_L} < 130$ GeV, when the lighter chargino mass is around 90 GeV. Fig. 12 shows that the total χ^2 improves slightly by including the $\Delta\overline{\delta}_G/\alpha$ correction to the muon decay, $\chi^2_{\rm tot}\ (\text{with}\Delta\overline{\delta}_G) < \chi^2_{\rm tot}\ (\text{without}\Delta\overline{\delta}_G)$, when $m_{\tilde{l}_L} \lesssim 130$ GeV and $\Delta\overline{\delta}_G < 0$.

Fig. 13 shows the slepton contributions to $R_\ell, A_e, A^\ell_{\rm FB}$ when $\tan\beta = 2$ and the lighter chargino mass is around 90 GeV ($\mu = 300$ GeV$, M_2 = 120$ GeV). In order to find the impact of the right-handed slepton on the observables, we show the cases of $m_{\tilde{l}_R} = 100$ GeV and $m_{\tilde{l}_R} = 1$ TeV by solid and dotted lines, respectively. We find that the non-oblique corrections from the slepton-ino loops are generally small and that they cannot remedy the unfavorable oblique effects of light left-handed sleptons. On the other hand, the right-handed slepton mass $m_{\tilde{l}_R}$ is not constrained significantly by the electroweak data.

6 Summary and Discussions

In this paper, we studied radiative corrections to the electroweak observables due to new particles in the MSSM systematically, confronting them against the latest data on the Z-boson parameters and the W-boson mass. After introducing our analytic framework and giving parametrizations of the SM predictions, we first studied the effects of the oblique (gauge-boson-propagator) corrections from squarks and sleptons (sec. 4.1), the MSSM Higgs bosons (sec. 4.2), charginos and neutralinos (sec. 4.3), separately. The effects of non-oblique corrections are then studied systematically; the MSSM Higgs-boson contributions to the Zbb and $Z\tau\tau$ vertices (sec. 5.1), the gluino-squark-loop corrections to the Zqq vertices (sec. 5.2), the squark-chargino/neutralino-loop corrections to the Zqq vertices (sec. 5.3), and the slepton-chargino/neutralino-loop corrections to the Zll vertices and the muon-decay amplitude (sec. 5.4). When studying contribution of each sector of the MSSM, we set all the irrelevant new particle masses sufficiently high so that their contributions can be neglected.

Our observations can be summarized as follows. The agreement between the SM predictions, and the electroweak data of Table 1 is excellent: for instance, the four-parameter fit (2.27) to the 22 data points of Table 1 (18 Z-parameters,

$m_W, m_t, \alpha_s(m_Z)$ and $\alpha(m_Z^2)$ [30]) finds $\chi^2_{\rm min}/({\rm d.o.f.}) = 18.2/(22-4)$, with the probability 44%. However, close examination of the fit shows that the data favor additional small negative contributions to the two oblique parameters, S_Z and T_Z: see Fig. 1. Small positive contribution to m_W can also improve the fit slightly if $m_t < 175$ GeV: see Fig. 2.

Our study of the oblique corrections in the MSSM can be summarized as follows by using, as a measure of the goodness of the MSSM fit as compared to the SM fit, the quantity

$$\Delta\chi^2 \equiv (\chi^2_{\rm tot})_{\rm MSSM} - (\chi^2_{\rm tot})_{\rm SM}, \tag{6.1}$$

where we compare the two fits by using the common parameter set (m_t(GeV), $1/\alpha(m_Z^2)$, $\alpha_s(m_Z)$)=(175, 128.90, 0.118) at $m_{H_{\rm SM}} = m_h = 100$ GeV.

- Small left-handed slepton mass ($m_{\widetilde{l}_L}$) makes ΔS_Z negative while keeping ΔT_Z essentially unchanged. It contribute positively to Δm_W. The fit worsens slightly ($\Delta\chi^2 \gtrsim 1$) if $m_{\widetilde{l}_L} \lesssim 170$ GeV for $\tan\beta = 2$ or $m_{\widetilde{l}_L} \lesssim 250$ GeV for $\tan\beta = 50$, and significantly ($\Delta\chi^2 \gtrsim 4$) if $m_{\widetilde{l}_L} \lesssim 110$ GeV for $\tan\beta = 2$ of $m_{\widetilde{l}_L} \lesssim 150$ GeV for $\tan\beta = 50$.

- Small left-handed squark mass parameters ($m_{\widetilde{Q}}, m_{\widetilde{Q}_3}$) make ΔT_Z and Δm_W positive while keeping ΔS_Z essentially unchanged. The effective $\widetilde{t}_L$-$\widetilde{t}_R$ mixing parameter $A^t_{\rm eff}$ of the magnitude of the order of $m_{\widetilde{Q}_3}$ tame the unfavorable positive ΔT_Z contribution, but not completely. The fit worsens significantly ($\Delta\chi^2 \gtrsim 4$) if $m_{\widetilde{Q}}(= m_{\widetilde{Q}_3}) \lesssim 340$ GeV for $\tan\beta = 2$ or $m_{\widetilde{Q}}(= m_{\widetilde{Q}_3}) \lesssim 300$ GeV for $\tan\beta = 50$, even for $A_{\rm eff} = 300$ GeV, which correspond to $m_{\widetilde{t}_1} \lesssim 300$ GeV ($\tan\beta = 2$) and $m_{\widetilde{t}_1} \lesssim 260$ GeV ($\tan\beta = 50$).

- The MSSM Higgs boson contribution can be approximated by the SM Higgs boson contribution at $m_{H_{\rm SM}} = m_h$ if the pseudo-scalar Higgs-boson mass satisfies $m_A \gtrsim 200$ GeV. The effects on the electroweak observables are small, $|\Delta\chi^2| \lesssim 1$ for $\tan\beta = 2$ or $|\Delta\chi^2| \lesssim 0.5$ for $\tan\beta = 50$, when the direct search bound of $m_h > 75$ GeV (3.6c) is taken into account. See Fig. 5 and Table 3.

- In contrast, the light charginos and neutralinos are found to contribute negatively to both ΔS_Z and ΔT_Z, while they contribute negligibly to Δm_W. Their contribution can hence improve the SM fit ($\Delta\chi^2 \sim -1$): see Figs. 6 and 7.

We find that the best fit is obtained when the lightest chargino mass ($m_{\widetilde{\chi}_1^-}$) is near its experimental lower bound, $m_{\widetilde{\chi}_1^-} \sim 90$ GeV, see Tables 4 and 5. Overall picture of the oblique corrections in the MSSM is summarized in Fig. 8.

Non-oblique corrections in the MSSM are then studied systematically in section 5 as follows. The MSSM Higgs bosons can affect the Zbb, $Z\tau\tau$ and $Z\nu_\tau\nu_\tau$ vertices through their Yukawa couplings to quarks and leptons of the third generation (sec. 5.1). The SUSY-QCD corrections to the Zqq vertices are studied when both squarks and gluinos are light (sec. 5.2). The contributions of the light squarks and light charginos/neutralinos to the Zqq vertices are then studied (sec. 5.3). When both sleptons and charginos/neutralinos are light, not only the Zll vertices but also the muon-decay amplitude is affected (sec. 5.4). We find:

- The vertex corrections due to the MSSM Higgs bosons can be significant ($\Delta\chi^2 \gtrsim 4$) if the pseudo-scalar Higgs-boson mass m_A is smaller than about 100 GeV for $\tan\beta \sim 1$. For $\tan\beta \sim 50$, the effects are significant when $m_A \lesssim 300$ GeV. The overall fit to the electroweak observables can only be worse than the SM: see Fig. 9.

- The order α_s SUSY-QCD corrections to the Zqq vertices are found to be negligibly small ($|\Delta\chi^2| \lesssim 0.5$) when squarks and gluino masses are bigger than about 200 GeV: see Fig. 10 and Table. 6.

- The Zqq vertex corrections due to light squarks and light charginos/neutralinos are found to be insignificant if we take into account the direct search mass bounds on the lightest squarks (3.4) and the lightest chargino (3.5). We also found that good overall fit to the electroweak data with $m_{\widetilde{\chi}_1^-} \sim 100$ GeV can be maintained with $m_{\widetilde{t}_1} \sim 100$ GeV if the left-handed squark mass is kept large, $m_{\widetilde{Q}} (= m_{\widetilde{Q}_3}) \gtrsim 1$ TeV: see Fig. 11.

- When the left-handed slepton mass is small ($m_{\widetilde{l}_L} \lesssim 200$ GeV) and charginos/neutralinos are light ($m_{\widetilde{\chi}_1^-} \sim 100$ GeV), the Zll vertices as well as the muon-decay amplitude are affected significantly. Although we find that their contribution to the muon-decay amplitude can improve the fit when $m_{\widetilde{l}_L} \sim 100$ GeV, its unfavorable oblique contributions make the overall fit worse than the SM ($\Delta\chi^2 \gtrsim 1$) for $m_{\widetilde{l}_L} \lesssim 150$ GeV.

Summing up, we find that no contribution of the MSSM particles can improve the fit to the electroweak data by taking into account the non-oblique corrections to the Zff vertices and the muon-decay amplitude. Best fit to the data is found when the supersymmetric fermions (charginos and neutralinos) are light, $m_{\widetilde{\chi}_1^-} \sim 100$ GeV, and the five scalar mass parameters $m_A, m_{\widetilde{L}}, m_{\widetilde{L}_3}, m_{\widetilde{Q}}$ and $m_{\widetilde{Q}_3}$ are all large; $m_A \gtrsim 300$ GeV, $m_{\widetilde{L}} = m_{\widetilde{L}_3} \gtrsim 500$ GeV, $m_{\widetilde{Q}} = m_{\widetilde{Q}_3} \gtrsim 1$ TeV. The singlet scalar-mass parameters, $m_{\widetilde{U}}, m_{\widetilde{U}_3}, m_{\widetilde{D}}, m_{\widetilde{D}_3}, m_{\widetilde{E}}$ and $m_{\widetilde{E}_3}$ do not affect the electroweak fit significantly, and hence light $\mathrm{SU}(2)_L$-singlet scalar bosons are allowed.

Before closing, we give a few examples of the MSSM predictions for all the 19 electroweak observables of Table 1 when we have light charginos/neutralinos ($m_{\widetilde{\chi}_1^-} \sim 100$ GeV) and relatively light singlet squarks and sleptons. We examine the four cases I to IV of Table 7, all of which have a light chargino of about 100 GeV and the lightest squark at around 200 GeV, and the lightest slepton at around 150 GeV. For brevity, we assumed that the SUSY breaking scalar masses, $m_{\widetilde{Q}}, m_{\widetilde{U}}, m_{\widetilde{D}}, m_{\widetilde{L}}, m_{\widetilde{E}}$ are universal among different generations, and the effective left-right mixing mass parameters of $\widetilde{t}, \widetilde{b}$ and $\widetilde{\tau}$, $A^t_{\text{eff}}, A^b_{\text{eff}}, A^\tau_{\text{eff}}$, are also common. The doublet squarks and sleptons are kept heavy at around 1 TeV and the pseudo-scalar Higgs-boson mass m_A is set at around 500 GeV in all four cases. The scenarios I and II are for $\tan\beta = 2$, III and IV are for $\tan\beta = 50$. $\mu = 300$ GeV for I and III while $\mu = -300$ GeV for II and IV. Masses of most relevant physical states are also shown in Table 7. Because $M_2 < |\mu|$ in all four cases, the lightest charginos/neutralinos are dominantly gauginos. The lightest squarks and sleptons of the third generation squarks and sleptons all have predominantly right-handed component. The gluino mass ($M_{\widetilde{g}} = M_3$) and the $\mathrm{U}(1)_Y$ gaugino mass M_1 are fixed by the 'unification' condition $M_3/M_2/M_1 = \hat{\alpha}_3/\hat{\alpha}_2/\hat{\alpha}_1$.

The predictions are compared with the data in Table 8 for the scenarios I and II ($\tan\beta = 2$) and in Table 9 for the scenarios III and IV ($\tan\beta = 50$). In each Table we give the reference SM predictions at $m_t = 175$ GeV and $m_{H_{\text{SM}}} = 100$ GeV for comparison. The first column in each scenario shows the contributions of charginos/neutralinos and the MSSM Higgs bosons only. The results of this column represent the predictions of the MSSM when all new particles except the charginos/neutralinos and the Higgs bosons are heavy. In the second column, we show the predictions when only the oblique corrections from the squarks and sleptons are added, and in the last column we show the complete MSSM predictions including all the vertex and box corrections. We show in the second column the predictions of the oblique corrections only in order to show the quantitative importance of non-oblique corrections.

From Table 8, we find that the MSSM predictions are almost completely determined by the oblique contributions of charginos and neutralinos in the scenarios I and II with $\tan\beta = 2$, where the three scalar-mass parameters, $m_A, m_{\widetilde{Q}}$ and $m_{\widetilde{L}}$ are all kept large. The relatively light squarks and sleptons of a few hundred GeV barely contribute to oblique or non-oblique corrections. In contrast, the $\tan\beta = 50$ cases of III and IV given in Table 9 show that the non-oblique corrections can have significant effects even though the physical mass spectrum in all four cases are similar in Table 7. This is because the enhanced Yukawa coupling of the b-quark allows the relatively light $\widetilde{b}_1$ of predominantly right-handed component to contribute to the Zbb vertices. This affects Γ_b (and hence R_b in Table 9) and Γ_h (and hence R_ℓ). Similar contributions to the $Z\tau_L\tau_L$ vertex are found not to affect

	Inputs									
	$\tan\beta$	μ	M_2	A_t	m_A	$m_{\widetilde{Q}}$	$m_{\widetilde{U}}$	$m_{\widetilde{D}}$	$m_{\widetilde{L}}$	$m_{\widetilde{E}}$
I	2	300	125	−657	486	956	196	181	894	129
II	2	−300	90	568	434	1273	183	176	639	159
III	50	300	110	812	481	1091	221	204	925	165
IV	50	−300	105	−657	486	956	196	181	894	129
	Outputs									
	m_h	$m_{\widetilde{\chi}_1^-}$	$m_{\widetilde{\chi}_1^0}$	$M_{\widetilde{g}}$	$m_{\widetilde{\tau}_1}$	$m_{\widetilde{\nu}}$	$m_{\widetilde{t}_1}$	$m_{\widetilde{b}_1}$	$m_{\widetilde{u}_R}$	$m_{\widetilde{d}_R}$
I	104	98.2	53.4	439	134	893	214	182	194	182
II	109	101	48.3	316	162	637	231	177	180	177
III	130	101	53.6	386	169	922	247	196	219	206
IV	128	98.4	51.7	369	133	892	230	168	193	183

Table 7: Inputs and outputs parameters of the MSSM scenarios I to IV with light charginos/neutralinos and light squarks and sleptons.

the fit significantly.

Finally, we would like to perform the '*global*' fit to all the electroweak data of Table 1 in the MSSM, by taking into account the present data on m_t (2.25a), $1/\alpha(m_Z^2)$ (2.25b) and $\alpha_s(m_Z)$ (2.25c). From the previous comprehensive studies, it is clear that the improvement of the total χ^2 over the SM can be realized only when a light (~ 100 GeV) chargino exists and when the left-handed squark and slepton masses ($m_{\widetilde{Q}}$ and $m_{\widetilde{L}}$) and the pseudo-scalar Higgs-boson mass (m_A) are all sufficiently large. In the following study, we assume that the universality of the scalar mass parameters among the different generations, $m_{\widetilde{Q}} = m_{\widetilde{Q}_3}$, $m_{\widetilde{U}} = m_{\widetilde{U}_3}$, $m_{\widetilde{D}} = m_{\widetilde{D}_3}$, $m_{\widetilde{L}} = m_{\widetilde{L}_3}$ and $m_{\widetilde{E}} = m_{\widetilde{E}_3}$. Also, we fix all the scalar mass parameters at 1 TeV ($m_{\widetilde{Q}} = m_{\widetilde{L}} = m_{\widetilde{U}} = m_{\widetilde{D}} = m_{\widetilde{E}} = m_A = 1$ TeV) and $A^f_{\rm eff} = 0$ for brevity. Then, there are three parameters left in the MSSM, $\tan\beta$, M_2 and μ. We find the total χ^2 as a function of the lighter chargino mass $m_{\widetilde{\chi}_1^-}$ for $\tan\beta = 2$ (Fig. 14) and $\tan\beta = 50$ (Fig. 15). Since it is worth studying how the mixing between the gaugino and the higgsino affects the fit, we show the following three cases separately: $M_2/\mu = 0.1$ (solid lines), 1 (dotted lines) and 10 (dashed lines). The small number of M_2/μ implies that the lighter chargino is dominantly the wino while the large number of M_2/μ implies that it is dominantly the higgsino. The behavior of $\chi^2_{\rm tot}$ in the small $m_{\widetilde{\chi}_1^-}$ region ($\lesssim 60$ GeV) can be understood from the chargino contribution to the R parameter, eq. (4.13), which behaves as $1/\beta$ when $m_{\widetilde{\chi}_1^-}$ is close to a half of m_Z.

In our assumption on the mass spectrum of the MSSM, the lightest Higgs boson mass is predicted as $m_h = 106$ GeV for $\tan\beta = 2$ and $m_h = 129$ GeV for $\tan\beta = 50$. The decoupling in the large SUSY mass limit is examined by

	Pull						
	SM*	I			II		
		inos/Higgs	obl.	all	inos/Higgs	obl.	all
Γ_Z	−1.4	−0.9	−1.0	−1.1	−0.9	−1.0	−1.1
σ_h^0	0.3	0.3	0.3	0.3	0.3	0.3	0.2
R_ℓ	0.7	0.8	0.8	0.7	0.8	0.8	0.7
$A_{\rm FB}^{0,\ell}$	0.3	0.5	0.5	0.5	0.5	0.5	0.4
R_e	0.7	0.7	0.7	0.7	0.7	0.7	0.7
R_μ	1.3	1.3	1.3	1.3	1.3	1.3	1.2
R_τ	−0.7	−0.6	−0.6	−0.6	−0.6	−0.6	−0.7
$A_{\rm FB}^{0,e}$	−0.5	−0.4	−0.4	−0.4	−0.4	−0.4	−0.4
$A_{\rm FB}^{0,\mu}$	−0.1	0.0	0.0	0.0	0.0	0.0	0.0
$A_{\rm FB}^{0,\tau}$	1.1	1.2	1.1	1.1	1.1	1.1	1.1
A_τ	−1.2	−1.0	−1.0	−1.0	−1.0	−1.1	−1.1
A_e	−0.1	0.1	0.0	0.1	0.0	0.0	0.0
R_b	1.2	1.2	1.2	1.1	1.2	1.2	1.0
R_c	0.3	0.3	0.3	0.3	0.3	0.3	0.3
$A_{FB}^{0,b}$	−2.4	−2.1	−2.2	−2.1	−2.2	−2.2	−2.2
$A_{FB}^{0,c}$	−0.8	−0.7	−0.7	−0.7	−0.7	−0.7	−0.7
$\sin^2\theta_{\rm eff}^{\rm lept}$	0.7	0.7	0.7	0.7	0.7	0.7	0.7
A_{LR}^0	1.0	1.4	1.3	1.3	1.3	1.3	1.2
A_b	−1.9	−1.9	−1.9	−1.9	−1.9	−1.9	−1.9
A_c	−0.5	−0.5	−0.5	−0.5	−0.5	−0.5	−0.5
m_W	0.2	0.1	0.1	0.1	0.1	0.1	0.1
$\chi^2_{\rm tot}$	19.8	18.1	18.2	18.1	18.2	18.3	18.2

Table 8: The pull factors of the predictions of the MSSM scenarios I and II. Those of the reference SM predictions (see Table. [11]) are given for comparison.

	Pull						
	SM*	III			IV		
		inos/Higgs	obl.	all	inos/Higgs	obl.	all
Γ_Z	−1.4	−0.8	−0.8	−0.8	−0.8	−0.8	−0.7
σ_h^0	0.3	0.3	0.3	0.2	0.3	0.3	0.1
R_ℓ	0.7	0.8	0.8	1.1	0.8	0.8	1.1
$A_{\mathrm{FB}}^{0,\ell}$	0.3	0.6	0.6	0.6	0.6	0.6	0.6
R_e	0.7	0.8	0.8	0.9	0.8	0.8	0.9
R_μ	1.3	1.3	1.3	1.5	1.3	1.3	1.6
R_τ	−0.7	−0.6	−0.6	−0.5	−0.6	−0.6	−0.5
$A_{\mathrm{FB}}^{0,e}$	−0.5	−0.4	−0.4	−0.4	−0.4	−0.4	−0.4
$A_{\mathrm{FB}}^{0,\mu}$	−0.1	0.1	0.1	0.1	0.1	0.1	0.1
$A_{\mathrm{FB}}^{0,\tau}$	1.1	1.2	1.2	1.2	1.2	1.2	1.2
A_τ	−1.2	−0.9	−0.9	−0.8	−0.9	−0.9	−0.9
A_e	−0.1	0.2	0.2	0.2	0.2	0.1	0.1
R_b	1.2	1.2	1.2	1.4	1.2	1.2	1.5
R_c	0.3	0.3	0.3	0.3	0.3	0.3	0.3
$A_{FB}^{0,b}$	−2.4	−1.9	−2.0	−2.1	−2.0	−2.0	−2.1
$A_{FB}^{0,c}$	−0.8	−0.6	−0.6	−0.6	−0.6	−0.6	−0.6
$\sin^2\theta_{\mathrm{eff}}^{\mathrm{lept}}$	0.7	0.6	0.6	0.6	0.6	0.6	0.6
A_{LR}^0	1.0	1.6	1.6	1.6	1.5	1.5	1.5
A_b	−1.9	−1.9	−1.9	−2.0	−1.9	−1.9	−2.0
A_c	−0.5	−0.5	−0.5	−0.5	−0.5	−0.5	−0.5
m_W	0.2	0.3	0.3	0.3	0.3	0.2	0.2
χ^2_{tot}	19.8	17.8	17.8	19.4	17.7	17.8	19.7

Table 9: The pull factors of the predictions of the MSSM scenarios III and IV. Those of the reference SM predictions (see Table. [11]) are given for comparison.

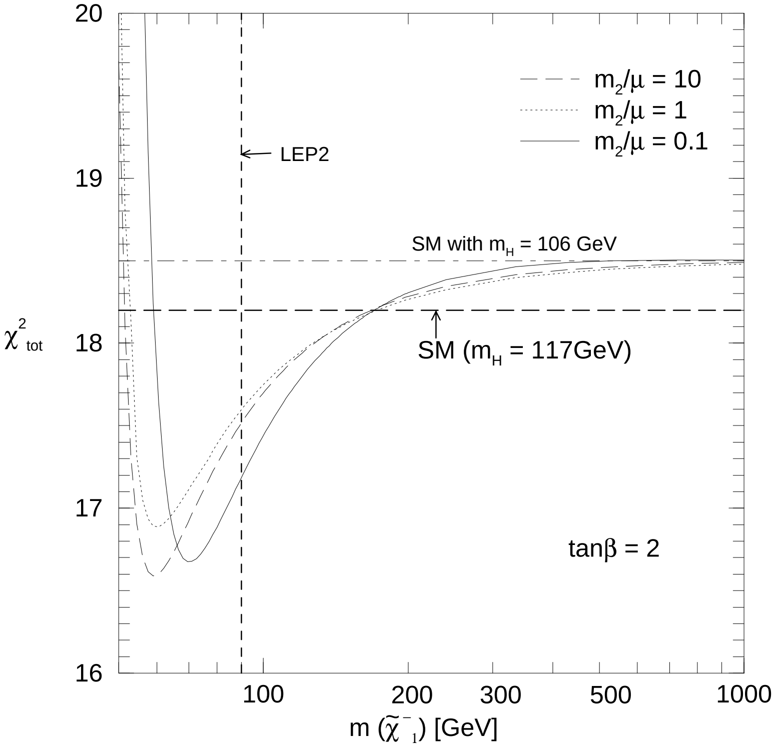

Figure 14: The total χ^2 in the MSSM as a function of the lighter chargino mass $m_{\tilde{\chi}_1^-}$ for $\tan\beta = 2$. The SM best fit ($\chi^2 = 18.2$) is shown by the dashed horizontal line. The dot-dashed horizontal line shows the SM fit using $m_{H_{\rm SM}} = 106$ GeV which is the lightest Higgs boson mass predicted in the MSSM. Three different M_2-μ ratio (10, 1, 0.1) are studied. The bound on $m_{\tilde{\chi}_1^-}$ from the LEP2 experiment is shown by the dashed vertical line.

comparing the MSSM fit with the SM fit at $m_{H_{\rm SM}} = m_h$ rather than the SM best fit at $m_{H_{\rm SM}} = 117$ GeV. We show by horizontal lines the corresponding SM results in Figs. 14 and 15. The decoupling seems to hold at $m_{\tilde{\chi}_1^-} = 1$ TeV for $\tan\beta = 2$. On the other hand, the MSSM prediction at $\tan\beta = 50$ differs slightly with the SM prediction at $m_{H_{\rm SM}} = m_h$ even when $m_{\tilde{\chi}_1^-} = 1$ TeV, as seen from Fig. 15. We looked for the origin of this small discrepancy and found that it comes from the non-oblique corrections as shown in Table 10. Among the 14 distinct Zff vertices of the MSSM that appear in eq. (2.5), we find that the Zb_Rb_R vertex receives the non-negligible corrections at $\tan\beta \sim 50$. Its origin is the enhanced Yukawa coupling among the b-quark, the t-quark and the heavy Higgs bosons $(A, H, H^\pm)$ of 1 TeV mass. In particular, the charged Higgs boson contributes to the Zb_Rb_R vertex has an additional enhancement factor due to the exchanged top-quark mass. The Yukawa couplings among the charged Higgs boson, the right-handed b-quark and the left-handed t-quark is proportional to $m_b \tan\beta$, which gives the largest coupling

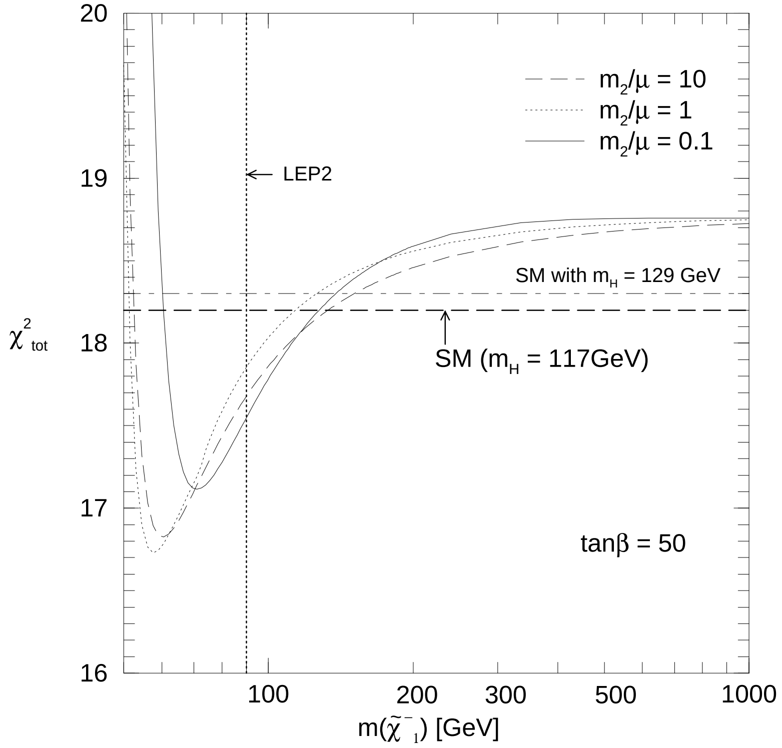

Figure 15: The total χ^2 in the MSSM as a function of the lighter chargino mass $m_{\tilde{\chi}_1^-}$ for $\tan\beta = 50$. The SM best fit ($\chi^2 = 18.2$) is shown by the dashed horizontal line. The dot-dashed horizontal line shows the SM fit using $m_{H_{\rm SM}} = 129$ GeV which is the lightest Higgs boson mass predicted in the MSSM. Three different M_2-μ ratio (10, 1, 0.1) are studied. The bound on $m_{\tilde{\chi}_1^-}$ from the LEP2 experiment is shown by the dashed vertical line.

in the MSSM when $\tan\beta > \sqrt{m_t/m_b} \approx 7$. The combined effects make the effective Zb_Rb_R coupling smaller than the SM by about 0.6% even when $m_{H^-} \approx 1$ TeV. This 0.6% decrease in g_R^b slightly worsen the fit to the R_b and $A_{\rm FB}^{0,b}$ data.

Taking account of the direct search limit on the chargino mass from LEP2, we can conclude that $m_{\tilde{\chi}_1^-} \sim 100$ GeV gives the best fit point of the MSSM in both small and large $\tan\beta$. Among the three ratios of M_2/μ, the gaugino dominant case ($M_2/\mu = 0.1$) gives slightly better fit at $m_{\tilde{\chi}_1^-} \sim 100$ GeV rather than the others. The improvement of the MSSM fit over the SM is not very significant, however, since the SM fit to the data is already good.

	$\tan\beta = 2$		$\tan\beta = 50$	
	obl.	obl. + vtx.	obl.	obl. + vtx.
χ^2_{min}	18.5	18.5	18.3	18.7
χ^2_{SM} at $m_{H_{\text{SM}}} = m_h$	—	18.5	—	18.3

Table 10: χ^2_{min} in the MSSM for $\tan\beta = 2$ and 50 which are estimated by using the oblique corrections only (obl.) and all the MSSM corrections (obl. + vtx.). All the scalar mass parameters are the same with those in Figs. 14 and 15. We take $M_2/\mu = 0.1$ as an example. As a reference, χ^2 in the SM (χ^2_{SM}) are shown for $m_{H_{\text{SM}}} = 106$ GeV and $m_{H_{\text{SM}}} = 129$ GeV, which should each correspond to the decoupling limit of the $\tan\beta = 2$ and $\tan\beta = 50$ cases, respectively.

7 Conclusion

We have presented the results of our comprehensive study of the constraints on the MSSM parameters from the electroweak precision measurements. The gauge-boson-propagator (oblique) corrections are parametrized in terms of three parameters, $\Delta S_Z, \Delta T_Z$ and Δm_W. The S_Z parameter is obtained from the standard S parameter by taking into account the running effect of the Z-boson propagator correction between $q^2 = 0$ and $q^2 = m_Z^2$, which we denoted by R, while the T_Z parameter is obtained from the standard T parameter by taking account of the R parameter and $\Delta\overline{\delta}_G$, which is the correction to the muon-decay amplitude. We found that the left-handed sfermion contributions always make the fit worse than the SM due to the positive contributions to the T_Z parameter (squarks) or the negative contributions to the S_Z parameter (sleptons). The contributions from the right-handed sfermions to the oblique parameters are negligible. The contributions of the MSSM Higgs bosons to the oblique parameters behave like the SM Higgs boson contribution at $m_{H_{\text{SM}}} = m_h$ when the pseudo-scalar Higgs-boson mass m_A is large ($m_A \gtrsim 300$ GeV). The most important finding of our study is that the light chargino contribution can make the fit better than that of the SM due to its effect on the R parameter. We therefore studied vertex and box corrections that contain light charginos/neutralinos and find that no combination of squarks and sleptons can improve the fit further.

The '*global*' fit of the MSSM has been performed by assuming the heavy mass limit of all the sfermions and the pseudo-scalar Higgs boson. We found that the best fit is obtained when the chargino mass is at the current lower bound from the LEP2 experiments.

Acknowledgment

The work of G.C.C. is supported in part by Grant-in-Aid for Scientific Research from the Ministry of Education, Science and Culture of Japan. K.H. thanks the JSPS-NSF Joint Research Project and the Phenomenology Institute of University of Wisconsin-Madison, for their hospitality while part of this work was done.

Note added

After submission of this paper, we learned that Djouadi *et al.* [44] calculated the two-loop QCD corrections to the gauge boson two-point functions. They found that the QCD correction enhances the one-loop squark contributions to the ρ-parameter (the T-parameter in our paper) by 10%–30%. This effect may shift effectively the stop mass in our results slightly higher. We would like to thank S. Heinemeyer for calling our attention to Ref. [44].

We also learned that it is not appropriate to use the experimental data on the effective weak mixing angle, $\sin^2\theta_{\rm eff}^{\rm lept}$ (see Table 1) which is measured from the jet-charge asymmetry, in our analysis when the non-universal vertex corrections are significant. This is because the parameter is obtained from the asymmetry data by assuming that the Z-boson decay branching fractions to each quark flavor obey the SM prediction. We confirm that our results presented in this paper do not change significantly when we remove the jet-charge asymmetry data in the fit. We are grateful to K. Moenig for clarifying the problem for us.

Appendix

A Mass eigenstates and couplings in the MSSM

All the analytic expressions for the 1-loop contributions of the MSSM particles are expressed in terms of the masses of the mass-eigenstates and their couplings. We summarize the notation of ref. [28] here for completeness.

The mixing matrix elements between the current-eigenstates and the mass-eigenstates appear in the expression for the gauge-boson-propagator corrections. There are four types of the mixing matrices in our restricted MSSM. For squarks and sleptons, we consider only the chirality mixing among the third generation squarks and sleptons:

$$\tilde{f}_L = \sum_{j=1}^{2} (U^{\tilde{f}})_{1j} \tilde{f}_j \,, \quad \tilde{f}_L^* = \sum_{j=1}^{2} (U^{\tilde{f}})^*_{1j} \tilde{f}_j^* \,, \tag{A.1a}$$

$$\tilde{f}_R = \sum_{j=1}^{2} (U^{\tilde{f}})_{2j} \tilde{f}_j \,, \quad \tilde{f}_R^* = \sum_{j=1}^{2} (U^{\tilde{f}})^*_{2j} \tilde{f}_j^* \,, \tag{A.1b}$$

for $\tilde{f} = \tilde{t}$, $\tilde{b}$ and $\tilde{\tau}$. For the charginos we have

$$\widetilde{W}_L^- = \sum_{j=1}^{2} (U_L^C)_{1j} \widetilde{\chi}_{jL}^- \,, \quad \widetilde{W}_R^+ = \sum_{j=1}^{2} (U_L^C)^*_{1j} \widetilde{\chi}_{jR}^+ \,, \tag{A.2a}$$

$$\widetilde{H}_{dL}^- = \sum_{j=1}^{2} (U_L^C)_{2j} \widetilde{\chi}_{jL}^- \,, \quad \widetilde{H}_{dR}^+ = \sum_{j=1}^{2} (U_L^C)^*_{2j} \widetilde{\chi}_{jR}^+ \,, \tag{A.2b}$$

$$\widetilde{W}_R^- = \sum_{j=1}^{2} (U_R^C)_{1j} \widetilde{\chi}_{jR}^- \,, \quad \widetilde{W}_L^+ = \sum_{j=1}^{2} (U_R^C)^*_{1j} \widetilde{\chi}_{jL}^+ \,, \tag{A.2c}$$

$$\widetilde{H}_{uR}^- = \sum_{j=1}^{2} (U_R^C)_{2j} \widetilde{\chi}_{jR}^- \,, \quad \widetilde{H}_{uL}^+ = \sum_{j=1}^{2} (U_R^C)^*_{2j} \widetilde{\chi}_{jL}^+ \,, \tag{A.2d}$$

and for the neutralinos we have

$$\widetilde{B}_L = \sum_{j=1}^{4} (U_L^N)_{1j} \widetilde{\chi}_{jL}^0 \,, \quad \widetilde{B}_R = \sum_{j=1}^{4} (U_R^N)_{1j} \widetilde{\chi}_{jR}^0 \,, \tag{A.3a}$$

$$\widetilde{W}_L^3 = \sum_{j=1}^{4} (U_L^N)_{2j} \widetilde{\chi}_{jL}^0 \,, \quad \widetilde{W}_R^3 = \sum_{j=1}^{4} (U_R^N)_{2j} \widetilde{\chi}_{jR}^0 \,, \tag{A.3b}$$

$$\widetilde{H}_{dL}^0 = \sum_{j=1}^{4} (U_L^N)_{3j} \widetilde{\chi}_{jL}^0 \,, \quad \widetilde{H}_{dR}^0 = \sum_{j=1}^{4} (U_R^N)_{3j} \widetilde{\chi}_{jR}^0 \,, \tag{A.3c}$$

$$\widetilde{H}_{uL}^0 = \sum_{j=1}^{4} (U_L^N)_{4j} \widetilde{\chi}_{jL}^0 \,, \quad \widetilde{H}_{uR}^0 = \sum_{j=1}^{4} (U_R^N)_{4j} \widetilde{\chi}_{jR}^0 \,. \tag{A.3d}$$

Finally, the Higgs bosons are expressed as follows:

$$H_u^+ = (H_u^-)^* = i\chi^+ \sin\beta + H^+ \cos\beta\,, \tag{A.4a}$$
$$H_d^- = (H_d^+)^* = i\chi^- \cos\beta + H^- \sin\beta\,, \tag{A.4b}$$
$$H_u^0 = \frac{1}{\sqrt{2}}(v\sin\beta + h\cos\alpha + H^0\sin\alpha - i\chi^3\sin\beta + iA\cos\beta)\,, \tag{A.4c}$$
$$H_d^0 = \frac{1}{\sqrt{2}}(v\cos\beta - h\sin\alpha + H^0\cos\alpha + i\chi^3\cos\beta + iA\sin\beta)\,. \tag{A.4d}$$

Here the phases α and β are fixed by requiring $\cos\beta, \sin\beta, \cos\alpha > 0$.

For notational compactness, we adopt the following generic notation of the MSSM couplings in Appendices C and D for the vertex and box corrections. Only three types of the couplings appear among the 9 types of the renormalizable couplings listed in ref. [28]. The FFV (fermion-fermion-vector) couplings, $g_\alpha^{F_1F_2V}$, are defined from the corresponding Lagrangian term as

$$\mathcal{L} = g_\alpha^{F_1F_2V}\overline{F_1}\gamma^\mu P_\alpha F_2 V_\mu \tag{A.5}$$

where $\alpha = L, R$. The SSV (scalar-scalar-vector) couplings, $g^{S_1S_2V}$, are defined by

$$\mathcal{L} = ig^{S_1S_2V} S_1^* \overleftrightarrow{\partial}_\mu S_2 V^\mu, \tag{A.6}$$

where $A\overleftrightarrow{\partial}_\mu B = A(\partial_\mu B) - (\partial_\mu A)B$. Finally, the FFS (fermion-fermion-scalar) couplings, $g_\alpha^{F_1F_2S}$, are defined by the following Lagrangian term:

$$\mathcal{L} = g_\alpha^{F_1F_2S}\overline{F_1}P_\alpha F_2 S, \tag{A.7}$$

where $\alpha = L$ or R. These simple rules determine uniquely the magnitude and the phases of the MSSM couplings that appear in Appendices C and D.

B Two point functions

B.1 Oblique parameters S, T, U, R

The transverse parts of the four gauge-boson-propagator functions are parametrized in ref. [23] as

$$\overline{\Pi}_T^{\gamma\gamma}(q^2) = \hat{e}^2\overline{\Pi}_T^{QQ}(q^2), \tag{B.1a}$$
$$\overline{\Pi}_T^{\gamma Z}(q^2) = \hat{e}\hat{g}_Z\Big\{\overline{\Pi}_T^{3Q}(q^2) - \hat{s}^2\overline{\Pi}_T^{QQ}(q^2)\Big\}, \tag{B.1b}$$
$$\overline{\Pi}_T^{ZZ}(q^2) = \hat{g}_Z^2\Big\{\overline{\Pi}_T^{33}(q^2) - 2\hat{s}^2\overline{\Pi}_T^{3Q}(q^2) + \hat{s}^4\overline{\Pi}_T^{QQ}(q^2)\Big\}, \tag{B.1c}$$
$$\overline{\Pi}_T^{WW}(q^2) = \hat{g}^2\overline{\Pi}_T^{11}(q^2), \tag{B.1d}$$

where $\hat{g}^2(\mu) = \hat{e}^2(\mu)/\hat{s}^2(\mu) = \hat{g}_Z^2(\mu)\hat{c}^2(\mu)$ are the $\overline{\text{MS}}$ couplings and all the polarization functions are renormalized in the $\overline{\text{MS}}$ scheme. The four effective charges are defined by

$$\frac{1}{\bar{e}^2(q^2)} = \frac{1}{\hat{e}^2(\mu)} + \mathrm{Re}\overline{\Pi}^{QQ}_{T,\gamma}(q^2), \tag{B.2a}$$

$$\frac{\bar{s}^2(q^2)}{\bar{e}^2(q^2)} = \frac{\hat{s}^2(\mu)}{\hat{e}^2(\mu)} + \mathrm{Re}\overline{\Pi}^{3Q}_{T,\gamma}(q^2), \tag{B.2b}$$

$$\frac{1}{\bar{g}_Z^2(q^2)} = \frac{1}{\hat{g}_Z^2(\mu)} + \mathrm{Re}\overline{\Pi}^{33}_{T,Z}(q^2) - 2\hat{s}^2\mathrm{Re}\overline{\Pi}^{3Q}_{T,Z}(q^2) + \hat{s}^4\mathrm{Re}\overline{\Pi}^{QQ}_{T,Z}(q^2), \tag{B.2c}$$

$$\frac{1}{\bar{g}_W^2(q^2)} = \frac{1}{\hat{g}^2(q^2)} + \mathrm{Re}\overline{\Pi}^{11}_{T,W}(q^2), \tag{B.2d}$$

where

$$\overline{\Pi}^{AB}_{T,V}(q^2) = \frac{\overline{\Pi}^{AB}_{T}(q^2) - \overline{\Pi}^{AB}_{T}(m_V^2)}{q^2 - m_V^2}, \tag{B.3}$$

and 'overline' denotes the inclusion of the pinch term [42]. The oblique correction terms are then expressed in terms of these effective charges and the weak boson masses [23];

$$\frac{S}{4} = \frac{\bar{s}^2(m_Z^2)\bar{c}^2(m_Z^2)}{\bar{\alpha}(m_Z^2)} - \frac{4\pi}{\bar{g}_Z^2(0)}, \tag{B.4a}$$

$$\alpha T = 1 - \frac{\bar{g}_W^2(0)}{m_W^2}\frac{m_Z^2}{\bar{g}_Z^2(0)}, \tag{B.4b}$$

$$\frac{S+U}{4} = \frac{\bar{s}^2(m_Z^2)}{\bar{\alpha}(m_Z^2)} - \frac{4\pi}{\bar{g}_W^2(0)}, \tag{B.4c}$$

$$R = \frac{16\pi}{\bar{g}_Z^2(0)} - \frac{16\pi}{\bar{g}_Z^2(m_Z^2)}, \tag{B.4d}$$

or of the reduced functions, $\overline{\Pi}^{QQ}_{T}(q^2), \overline{\Pi}^{3Q}_{T}(q^2), \overline{\Pi}^{33}_{T}(q^2)$ and $\overline{\Pi}^{11}_{T}(q^2)$:

$$S = 16\pi\mathrm{Re}\Big[\overline{\Pi}^{3Q}_{T,\gamma}(m_Z^2) - \overline{\Pi}^{33}_{T,Z}(0)\Big], \tag{B.5a}$$

$$T = \frac{4\sqrt{2}G_F}{\alpha}\Big[\overline{\Pi}^{33}_{T}(0) - \overline{\Pi}^{11}_{T}(0)\Big], \tag{B.5b}$$

$$U = 16\pi\mathrm{Re}\Big[\overline{\Pi}^{33}_{T,Z}(0) - \overline{\Pi}^{11}_{T,W}(0)\Big], \tag{B.5c}$$

$$\begin{aligned} R = 16\pi\Big[&\overline{\Pi}^{33}_{T,Z}(0) - \overline{\Pi}^{33}_{T,Z}(q^2) - 2\hat{s}^2\Big\{\overline{\Pi}^{3Q}_{T,Z}(0) - \overline{\Pi}^{3Q}_{T,Z}(q^2)\Big\} \\ &+ \hat{s}^4\Big\{\overline{\Pi}^{QQ}_{T,Z}(0) - \overline{\Pi}^{QQ}_{T,Z}(q^2)\Big\}.\Big] \end{aligned} \tag{B.5d}$$

The MSSM contribution to the S, T, U, R parameters are then calculable from the MSSM particle contributions to the four Π^{AB}_{T} functions. All the results listed below agree with those in ref. [26].

B.2 MSSM Higgs bosons

The MSSM Higgs boson contributions are summarized as follows:

$$16\pi^2\Pi_T^{QQ} = B_5(q^2 : m_{H^-}, m_{H^-}), \tag{B.6a}$$

$$16\pi^2\Pi_T^{3Q} = \frac{1}{2}B_5(q^2 : m_{H^-}, m_{H^-}), \tag{B.6b}$$

$$\begin{aligned}16\pi^2\Pi_T^{33} = \frac{1}{4}\Big[&\cos^2(\alpha-\beta)\{B_5(q^2 : m_h, m_A) + B_5(q^2 : m_Z, m_H)\} \\ &+ \sin^2(\alpha-\beta)\{B_5(q^2 : m_H, m_A) + B_5(q^2 : m_Z, m_h)\} + B_5(q^2 : m_{H^-}, m_{H^-})\Big] \\ &+ m_Z^2\Big[\sin^2(\alpha-\beta)B_0(q^2 : m_Z, m_h) + \cos^2(\alpha-\beta)B_0(q^2 : m_Z, m_H)\Big],\end{aligned} \tag{B.6c}$$

$$\begin{aligned}16\pi^2\Pi_T^{11} = \frac{1}{4}\Big[&\cos^2(\alpha-\beta)\{B_5(q^2 : m_{H^-}, m_h) + B_5(q^2 : m_W, m_H)\} \\ &+ \sin^2(\alpha-\beta)\{B_5(q^2 : m_{H^-}, m_H) + B_5(q^2 : m_W, m_h)\} + B_5(q^2 : m_A, m_{H^-})\Big] \\ &+ m_W^2\Big[\sin^2(\alpha-\beta)B_0(q : m_W, m_h) + \cos^2(\alpha-\beta)B_0(q : m_W, m_H)\Big].\end{aligned} \tag{B.6d}$$

The B-functions are defined in Appendix D in ref. [23]. The SM Higgs boson contribution is reproduced by removing all terms with H^-, H and A, and by setting $\sin^2(\alpha-\beta) = 1$ and $m_h = m_{H_{\rm SM}}$.

B.3 Scalar fermions

The scalar fermion contributions are summarized as:

$$16\pi^2\Pi_T^{QQ} = C_f Q_f^2 \sum_{\alpha=1}^{2} B_5(q^2 : m_{\widetilde{f}_\alpha}, m_{\widetilde{f}_\alpha}), \tag{B.7a}$$

$$16\pi^2\Pi_T^{3Q} = C_f Q_f I_{3f} \sum_{\alpha=1}^{2} |(U^{\widetilde{f}})_{\alpha 1}|^2 B_5(q^2 : m_{\widetilde{f}_\alpha}, m_{\widetilde{f}_\alpha}), \tag{B.7b}$$

$$16\pi^2\Pi_T^{33} = C_f I_{3f}^2 \sum_{\alpha,\beta=1}^{2} |(U^{\widetilde{f}})_{\alpha 1}|^2 |(U^{\widetilde{f}})_{\beta 1}|^2 B_5(q^2 : m_{\widetilde{f}_\alpha}, m_{\widetilde{f}_\beta}), \tag{B.7c}$$

$$16\pi^2\Pi_T^{11} = C_f \frac{1}{2} \sum_{\alpha,\beta=1}^{2} |(U^{\widetilde{u}})_{\alpha 1}|^2 |(U^{\widetilde{d}})_{\beta 1}|^2 B_5(q^2 : m_{\widetilde{u}_\alpha}, m_{\widetilde{d}_\beta}), \tag{B.7d}$$

where the color factor C_f is 3 for squarks and 1 for sleptons. The electric charge Q_f is given by $(2/3, -1/3, 0, -1)$ for $(\widetilde{u}, \widetilde{d}, \widetilde{\nu}_l, \widetilde{l})$. I_{3f} denotes the third component of the weak isospin: $+1/2, -1/2$ for the up- and down-type sfermions, respectively. The indices α, β take L, R for the first two generations (no left-right mixing) and $1, 2$ for the third generation. If there is no mixing between $\widetilde{f}_L$ and $\widetilde{f}_R$, the unitary matrix $(U^{\widetilde{f}})_{\alpha\beta}$ should be replaced by $\delta_{\alpha\beta}$.

B.4 Charginos and Neutralinos

The chargino and neutralino contributions are as follows:

$$16\pi^2\Pi_T^{QQ} = 8q^2 B_3(q^2 : m_{\widetilde{\chi}_i^-}, m_{\widetilde{\chi}_i^-}), \tag{B.8a}$$

$$16\pi^2\Pi_T^{3Q} = \left\{4 - \left|(U_L^C)_{2i}\right|^2 - \left|(U_R^C)_{2i}\right|^2\right\} 2q^2 B_3(q^2 : m_{\widetilde{\chi}_i^-}, m_{\widetilde{\chi}_i^-}), \tag{B.8b}$$

$$\begin{aligned} 16\pi^2\Pi_T^{33} = {} & \Big[2\Big\{|(D_L)_{ij}|^2 + |(D_R)_{ij}|^2\Big\}(2q^2 B_3 - B_4) \\ & + 2m_{\widetilde{\chi}_i^-} m_{\widetilde{\chi}_j^-}\Big\{(D_L)_{ij}(D_R)^*_{ij} + (D_L)^*_{ij}(D_R)_{ij}\Big\}B_0\Big](q^2 : m_{\widetilde{\chi}_i^-}, m_{\widetilde{\chi}_j^-}) \\ & + \Big[\Big\{|(N_L)_{ij}|^2 + |(N_R)_{ij}|^2\Big\}(2q^2 B_3 - B_4) \\ & + m_{\widetilde{\chi}_i^0} m_{\widetilde{\chi}_j^0}\Big\{(N_L)_{ij}(N_R)^*_{ij} + (N_L)^*_{ij}(N_R)_{ij}\Big\}B_0\Big](q^2 : m_{\widetilde{\chi}_i^0}, m_{\widetilde{\chi}_j^0}), \end{aligned} \tag{B.8c}$$

$$\begin{aligned} 16\pi^2\Pi_T^{11} = {} & 2\Big[\Big\{|(C_L)_{ij}|^2 + |(C_R)_{ij}|^2\Big\}(2q^2 B_3 - B_4)(q^2 : m_{\widetilde{\chi}_i^0}, m_{\widetilde{\chi}_j^-}) \\ & + m_{\widetilde{\chi}_i^0} m_{\widetilde{\chi}_j^-}\Big\{(C_L)_{ij}(C_R)^*_{ij} + (C_L)^*_{ij}(C_R)_{ij}\Big\}B_0(q^2 : m_{\widetilde{\chi}_i^0}, m_{\widetilde{\chi}_j^-})\Big], \end{aligned} \tag{B.8d}$$

where

$$(C_\alpha)_{ij} = (U_\alpha^N)^*_{2i}(U_\alpha^C)_{1j} + \frac{1}{\sqrt{2}}(U_\alpha^N)^*_{3i}(U_\alpha^C)_{2j}, \tag{B.9a}$$

$$(D_\alpha)_{ij} = (U_\alpha^C)^*_{1i}(U_\alpha^C)_{1j} + \frac{1}{2}(U_\alpha^C)^*_{2i}(U_\alpha^C)_{2j}, \tag{B.9b}$$

$$(N_L)_{ij} = -(N_R)^*_{ij} = \frac{1}{2}\Big\{(U_L^N)^*_{3i}(U_L^N)_{3j} - (U_L^N)^*_{4i}(U_L^N)_{4j}\Big\}. \tag{B.9c}$$

Here $\alpha = L$ or R in (B.9a) and (B.9b).

C Vertex corrections on $Z \to f_\alpha \overline{f_\alpha}$

Here we give the 1-loop corrections to the process $Z \to f_\alpha \overline{f_\alpha}$ in the MSSM. The radiative corrections to the effective coupling g_α^f is denoted by

$$\Delta g_\alpha^f = \frac{1}{\sqrt{4\sqrt{2} G_F m_Z^2}} \Big\{ g_\alpha^{ffZ} \Sigma'_{f_\alpha}(0) - \Gamma_{f_\alpha}(m_Z^2) \Big\}, \tag{C.1}$$

where $\Sigma'_{f_\alpha}(0)$ is the derivative of the self energy function of the external fermion f_α with the chirality $\alpha = L$ or R, whose mass is neglected:

$$\Sigma'_{f_\alpha}(0) = \frac{d}{dq^2} \Sigma_{f_\alpha}(q^2) \Big|_{q^2=0}. \tag{C.2}$$

We can express the self energy $\Sigma'_{f_\alpha}(0)$ and the vertex function $\Gamma_{f_\alpha}(q^2)$ mediated by a fermion ψ and a scalar ϕ in a compact generic notation as follows:

$$(4\pi)^2 \Sigma'_{f_\alpha}(0) = C_g \Big| g_\alpha^{\psi_j f \phi_i} \Big|^2 \Big(B_0 + B_1 \Big)(0 : m_{\phi_i}, m_{\psi_j}), \tag{C.3a}$$

$$\begin{aligned}(4\pi)^2 \Gamma_{f_\alpha}(q^2) = -C_g \Bigg\{ & \Big(g_\alpha^{\psi_j f \phi_k} \Big)^* g_\alpha^{\psi_i f \phi_k} \Big[g_\alpha^{\psi_j \psi_i Z} m_{\psi_i} m_{\psi_j} C_0 \\ & + g_{-\alpha}^{\psi_j \psi_i Z} \Big\{ -q^2 (C_{12} + C_{23}) - 2C_{24} + \frac{1}{2} \Big\} \Big] \\ & \times (p_1, p_2 : m_{\psi_i}, m_{\phi_k}, m_{\psi_j}) \\ & - \Big(g_\alpha^{\psi_k f \phi_i} \Big)^* g_\alpha^{\psi_k f \phi_j} g^{\phi_i \phi_j Z} 2C_{24}(p_1, p_2 : m_{\phi_j}, m_{\psi_k}, m_{\phi_i}) \Bigg\}. \end{aligned} \tag{C.3b}$$

Here C_g is 4/3 for the gluino contribution ($\psi = \widetilde{g}$) and 1 for the others. The chirality index $-\alpha$ follows the rule: $-L = R, -R = L$. For each external fermion f, the following combination of $\{\psi, \phi\}$ contribute to the vertices:

	$\{\psi, \phi\}$			
	$f = u$	d	ν_l	l
$\psi =$ chargino	$\{\widetilde{\chi}^+, \widetilde{d}_i^*\}$	$\{\widetilde{\chi}^-, \widetilde{u}_i^*\}$	$\{\widetilde{\chi}^+, \widetilde{l}_i^*\}$	$\{\widetilde{\chi}^-, \widetilde{\nu}_l^*\}$
$\psi =$ neutralino	$\{\widetilde{\chi}^0, \widetilde{u}_i^*\}$	$\{\widetilde{\chi}^0, \widetilde{d}_i^*\}$	$\{\widetilde{\chi}^0, \widetilde{\nu}_l^*\}$	$\{\widetilde{\chi}^0, \widetilde{l}_i^*\}$
$\psi =$ gluino	$\{\widetilde{g}, \widetilde{u}_i^*\}$	$\{\widetilde{g}, \widetilde{d}_i^*\}$	$-$	$-$
$\phi =$ charged Higgs	$\{d, H^-\}$	$\{u, H^+\}$	$\{l, H^-\}$	$\{\nu, H^+\}$
$\phi =$ neutral Higgs	$\{u, (h, H, A)\}$	$\{d, (h, H, A)\}$	$-$	$\{l, (h, H, A)\}$

(C.4)

The generic coupling notations of (A.5) – (A.7) then suffice to calculate all the $Z f_\alpha f_\alpha$ vertex corrections, Δg_α^f. Summation should be taken over all non-vanishing coupling combinations. When $d = b$ or $\ell = \tau$, the summations over the sfermion index is taken over $i = 1$ and 2. Otherwise, only the $i = \alpha$ sfermion contributes. We reproduced numerically the results reported in refs. [8, 9, 10].

D SUSY contributions to the μ-decay process

The μ-decay constant is parametrized in ref. [23] as

$$G_F = \frac{\bar{g}_W^2(0) + \hat{g}^2 \overline{\delta}_G}{4\sqrt{2} m_W^2}, \tag{D.1}$$

with

$$\overline{\delta}_G = (\overline{\delta}_G)_{\rm SM} + \Delta\overline{\delta}_G. \tag{D.2}$$

In the MSSM, $\Delta\overline{\delta}_G$ receives contributions from the vertex and the box diagrams

$$\Delta\overline{\delta}_G = 2\delta_g^{(v)} + \delta_g^{(b)}. \tag{D.3}$$

D.1 Vertex corrections

The $f_1 f_2 W$ vertex correction can be expressed as

$$g_L^{f_1 f_2 W} \delta^{(v)} = \Gamma^{f_1 f_2 W}(0) - \frac{1}{2} g_L^{f_1 f_2 W} \Big\{ \Sigma'_{f_1}(0) + \Sigma'_{f_2}(0) \Big\}. \tag{D.1}$$

In the $\mu \to \nu_\mu e \overline{\nu}_e$ process, the $\mu\nu_\mu W^-$ and $\nu_e e W^+$ vertices give the some $\delta^{(v)}$, with $g_L^{\mu\nu_\mu W^-} = g_L^{\nu_e e W^+} = \frac{\hat{g}}{\sqrt{2}}$. From the $\nu_e e W^+$ vertex, we find

$$(4\pi)^2 \Sigma'_{e_L}(0) = \left| g_L^{\widetilde{\chi}_i^0 e \widetilde{e}_L} \right|^2 (B_0 + B_1)(0 : m_{\widetilde{e}_L}, m_{\widetilde{\chi}_i^0}) + \left| g_L^{\widetilde{\chi}_j^- e \widetilde{\nu}_e} \right|^2 (B_0 + B_1)(0 : m_{\widetilde{\nu}_e}, m_{\widetilde{\chi}_j^-}), \tag{D.2a}$$

$$(4\pi)^2 \Sigma'_{\nu_e}(0) = \left| g_L^{\widetilde{\chi}_i^0 \nu_e \widetilde{\nu}_e} \right|^2 (B_0 + B_1)(0 : m_{\widetilde{\nu}_e}, m_{\widetilde{\chi}_i^0}) + \left| g_L^{\widetilde{\chi}_j^+ \nu_e \widetilde{e}_L} \right|^2 (B_0 + B_1)(0 : m_{\widetilde{e}_L}, m_{\widetilde{\chi}_j^-}), \tag{D.2b}$$

$$\begin{aligned}
(4\pi)^2 \Gamma_{e\nu_e W^+} = & -(g_L^{\widetilde{\chi}_j^+ \nu_e \widetilde{e}_L})^* g_L^{\widetilde{\chi}_i^0 e \widetilde{e}_L} \Big\{ g_L^{\widetilde{\chi}_j^+ \widetilde{\chi}_i^0 W} m_{\widetilde{\chi}_i^0} m_{\widetilde{\chi}_j^-} C_0 + g_R^{\widetilde{\chi}_j^+ \widetilde{\chi}_i^0 W} (-2C_{24} + \frac{1}{2}) \Big\} \\
& \qquad \times (0 : m_{\widetilde{\chi}_i^0}, m_{\widetilde{e}_L}, m_{\widetilde{\chi}_j^-}) \\
& -(g_L^{\widetilde{\chi}_i^0 \nu_e \widetilde{\nu}_e})^* g_L^{\widetilde{\chi}_j^- e \widetilde{\nu}_e} \Big\{ g_L^{\widetilde{\chi}_i^0 \widetilde{\chi}_j^- W} m_{\widetilde{\chi}_i^0} m_{\widetilde{\chi}_j^-} C_0 + g_R^{\widetilde{\chi}_i^0 \widetilde{\chi}_j^- W} (-2C_{24} + \frac{1}{2}) \Big\} \\
& \qquad \times (0 : m_{\widetilde{\chi}_j^-}, m_{\widetilde{\nu}_e}, m_{\widetilde{\chi}_i^0}) \\
& +(g_L^{\widetilde{\chi}_i^0 \nu_e \widetilde{\nu}_e})^* g_L^{\widetilde{\chi}_i^0 e \widetilde{e}_L} g_L^{\widetilde{\nu}_e \widetilde{e}_L W} 2C_{24}(0 : m_{\widetilde{e}_L}, m_{\widetilde{\chi}_i^0}, m_{\widetilde{\nu}_e}).
\end{aligned} \tag{D.3}$$

In eqs. (D.2), (D.3), summation over $i = 1$ to 4 ($\widetilde{\chi}_i^0$) and $j = 1$ to 2 ($\widetilde{\chi}_j^-$) should be understood. The momentum arguments of the C-functions are set to zero ($p_i^2 = p_i p_j = 0$).

D.2 Box corrections

The box contributions to the $\mu \to \nu_\mu e \overline{\nu}_e$ amplitude can be expressed as

$$iT = i\Big\{M(1) + M(2) + M(3) + M(4)\Big\}\overline{u_e}\gamma^\mu P_L v_{\nu_e}\overline{u_{\nu_\mu}}\gamma^\mu P_L u_\mu. \tag{D.4}$$

By taking into account the normalization of the tree-level amplitude, $-\hat{g}^2/2m_W^2$, the box diagram contributions to the $\overline{\delta}_G$ parameter is

$$\delta^{(b)} = -\frac{2m_W^2}{\hat{g}^2}\sum_{i=1}^{4} M(i). \tag{D.5}$$

Each $M(i)$ is given by

$$16\pi^2 M(1) = (g_L^{\widetilde{\chi}_i^0 e\widetilde{e}_L})^* g_L^{\widetilde{\chi}_i^0 \mu\widetilde{\mu}_L}(g_L^{\widetilde{\chi}_j^+ \nu_\mu\widetilde{\mu}_L})^* g_L^{\widetilde{\chi}_j^+ \nu_e\widetilde{e}_L} D_{27}(m_{\widetilde{\mu}_L}, m_{\widetilde{e}_L}, m_{\widetilde{\chi}_j^+}, m_{\widetilde{\chi}_i^0}) \tag{D.6a}$$

$$16\pi^2 M(2) = (g_L^{\widetilde{\chi}_j^- e\widetilde{\nu}_e})^* g_L^{\widetilde{\chi}_j^- \mu\widetilde{\nu}_\mu}(g_L^{\widetilde{\chi}_i^0 \nu_\mu\widetilde{\nu}_\mu})^* g_L^{\widetilde{\chi}_i^0 \nu_e\widetilde{\nu}_e} D_{27}(m_{\widetilde{\nu}_\mu}, m_{\widetilde{\nu}_e}, m_{\widetilde{\chi}_j^-}, m_{\widetilde{\chi}_i^0}) \tag{D.6b}$$

$$16\pi^2 M(3) = \frac{1}{2} m_{\widetilde{\chi}_i^0} m_{\widetilde{\chi}_j^-} g_L^{\widetilde{\chi}_j^+ \nu_e\widetilde{e}_L} g_L^{\widetilde{\chi}_j^- \mu\widetilde{\nu}_\mu}(g_L^{\widetilde{\chi}_i^0 \nu_\mu\widetilde{\nu}_\mu})^*(g_L^{\widetilde{\chi}_i^0 e\widetilde{e}_L})^* D_0(m_{\widetilde{\nu}_\mu}, m_{\widetilde{e}_L}, m_{\widetilde{\chi}_j^-}, m_{\widetilde{\chi}_i^0}) \tag{D.6c}$$

$$16\pi^2 M(4) = \frac{1}{2} m_{\widetilde{\chi}_i^0} m_{\widetilde{\chi}_j^-} g_L^{\widetilde{\chi}_i^0 \nu_e\widetilde{\nu}_e} g_L^{\widetilde{\chi}_i^0 \mu\widetilde{\mu}_L}(g_L^{\widetilde{\chi}_j^+ \nu_\mu\widetilde{\mu}_L})^*(g_L^{\widetilde{\chi}_j^- e\widetilde{\nu}_e})^* D_0(m_{\widetilde{\mu}_L}, m_{\widetilde{\nu}_e}, m_{\widetilde{\chi}_j^-}, m_{\widetilde{\chi}_i^0}) \tag{D.6d}$$

All the D-functions are evaluated at the zero momentum transfer limit. We reproduced the results presented in ref. [43].

References

[1] E. Witten, Nucl. Phys. **B188** (1981) 513;
S. Dimopoulos and H. Georgi, Nucl. Phys. **B193** (1981) 150;
N. Sakai, Z. Phys. **C11** (1981) 153.

[2] E. Gildner and S. Weinberg, Phys. Rev. **D13** (1976) 1333;
E. Gildner, Phys. Rev. **D14** (1976) 1667.

[3] S. Weinberg, Phys. Rev. **D19** (1979) 1277;
L. Susskind, Phys. Rev. **D20** (1979) 2619.

[4] K. Inoue, A. Kakuto, H. Komatsu and S. Takeshita, Prog. Theor. Phys. **68** (1982) 927; **70** (1983) 330 (E); Prog. Theor. Phys. **71** (1984) 413.

[5] L.E. Ibáñez and G.G. Ross, Phys. Lett. **B110** (1982) 215;
L.E. Ibáñez, Phys. Lett. **B118** (1982) 72;
J. Ellis, D.V. Nanopoulos and K. Tamvakis, Phys. Lett. **B121** (1983) 123;
L. Alvarez-Gaumé, J. Polchinski and M.B. Wise, Nucl. Phys. **B221** (1983) 495.

[6] C. Giunti, C.W. Kim and U.W. Lee, Mod. Phys. Lett. **A6** (1991) 1745;
U. Amaldi, W. de Boer and H. Fürstenau, Phys. Lett. **B260** (1991) 447;
P. Langacker and M. Luo, Phys. Rev. **D44** (1991) 817;
J. Ellis, S. Kelley and D.V. Nanopoulos, Phys. Lett. **B260** (1991) 131.

[7] The CDF Collaboration, Phys. Rev. **D50** (1994) 2966;
The CDF Collaboration, Phys. Rev. Lett. **74** (1995) 2626;
The D0 Collaboration, Phys. Rev. Lett. **74** (1995) 2632.

[8] K. Hagiwara and H. Murayama, Phys. Lett. **B246** (1990) 533;
A. Djouadi, M. Drees and H. Konig, Phys. Rev. **D48** (1993) 3081.

[9] M. Boulware and D. Finnell, Phys. Rev. **D44** (1991) 2054;
G. Altarelli, R. Barbieri and F. Caravaglios, Phys. Lett. **B314** (1993) 357;
J.D. Wells, C. Kolda and G.L. Kane, Phys. Lett. **B338** (1994) 219;
D. Garcia and J. Sola, Phys. Lett. **B354** (1995) 335;
D. Garcia, R.A. Jimenez and J. Sola, Phys. Lett. **B347** (1995) 309; Phys. Lett. **B347** (1995) 321; **B351** (1995) 602 (E).

[10] Y. Yamada, K. Hagiwara and S. Matsumoto, Prog. Theor. Phys. Suppl. **123** (1996) 195 (hep-ph/9512227);
J.D. Wells and G.L. Kane, Phys. Rev. Lett. **76** (1996) 869;

J. Ellis, J.L. Lopez and D. Nanopoulos, Phys. Lett. **B372** (1996) 95;
P.H. Chankowski and S. Pokorski, Nucl. Phys. **B475** (1996) 3.

[11] The LEP Collaborations ALEPH, DELPHI, L3, OPAL, the LEP Electroweak Working Group and the SLD Heavy Flavor Group, CERN-EP/99-15.

[12] Y. Okada, M. Yamaguchi and T. Yanagida, Prog. Theor. Phys. **85** (1991) 1;
H. Haber and R. Hempfling, Phys. Rev. Lett. **66** (1991) 1815;
J. Ellis, G. Ridorfi and F. Zwirner, Phys. Lett. **B257** (1991) 83.

[13] G.L. Kane, C. Kolda and J.D. Wells, Phys. Rev. Lett. **70** (1993) 2686;
D. Comeli and C. Verzegnassi, Phys. Rev. **D47** (1993) 764.

[14] J.A. Casas, J.R. Espinosa, M. Quiros and A. Riotto, Nucl. Phys. **B436** (1995) 3, (E) **B439** (1995) 466;
M. Carena, M. Quiros and C.E. Wagner, Nucl. Phys. **B461** (1996) 407;
H.E. Haber, R. Hempfling and A.H. Hoang, Z. Phys. **C75** (1997) 539.

[15] R. Hempfling and A.H. Hoang, Phys. Lett. **B331** (1994) 99;
R. Zhang, Phys. Lett. **B447** (1999) 89.

[16] S. Heinemeyer, W. Hollik and G. Weiglein, Phys. Lett. **B455** (1999) 179.

[17] R. Barbieri, M. Frigeni, F. Giuliani and H.E. Haber, Nucl. Phys. **B341** (1990) 309;
J. Ellis, G.L. Fogli and E. Lisi, Nucl. Phys. **B393** (1993) 3;
J.L. Lopez, D.V. Nanopoulos, G.T. Park, H. Pois and K.J Yuan, Phys. Rev. **D48** (1993) 3297;
J. Ellis, G.L. Fogli and E. Lisi, Phys. Lett. **B324** (1994) 173;
P.H. Chankowski, A. Dabelstein, W. Hollik, W.M. Mosle, S. Pokorski and J. Rosiek , Nucl. Phys. **B417** (1994) 101;
D. Garcia and J. Sola, Mod. Phys. Lett. **A9** (1994) 211;
G.L. Kane, R.G. Stuart and J.D. Wells, Phys. Lett. **B354** (1995) 350;
P.H. Chankowski and S. Pokorski, Phys. Lett. **B366** (1996) 188;
D.M. Pierce, J.A. Bagger, K. Matchev and R.J. Zhang, Nucl. Phys. **B491** (1997) 3;
M. Carena, P. Chankowski, M. Olechowski, S. Pokorski and C.E.M Wagner, Nucl. Phys. **B491** (1997) 103;
W. de Boer, A. Dabelstein, W. Hollik, W. Mösle, and U. Schwickerath, Z. Phys. **C75** (1997) 627;
P.H. Chankowski, J. Ellis and S. Pokorski, Phys. Lett. **B423** (1998) 327;
J. Erler and D.M Pierce, Nucl. Phys. **B526** (1998) 53;

P.H. Chankowski and S. Pokorski, "*Supersymmetric Loop Effects*" in "*Perspectives on supersymmetry*", p402, (ed) G.L. Kane, World Scientific, 1998 (hep-ph/9707497);
I.V. Gaidaenko, A.V. Novikov, V.A. Novikov, A.N. Rozanov and M.I. Vysotsky, hep-ph/9812346;
A. Dedes, A.B. Lahanas and K. Tamvakis, Phys. Rev. **D59** (1999) 015019.

[18] G.C. Cho, K. Hagiwara, C. Kao and R. Szalapski, Contribution to Physics at Run II: Workshop on Supersymmetry/Higgs: Summary Meeting, Fermilab, 19-21 Nov 1998 (hep-ph/9901351).

[19] M.E. Peskin and T. Takeuchi, Phys. Rev. Lett. **65** (1990) 964; Phys. Rev. **D46** (1992) 381.

[20] B. Holdom and J. Terning, Phys. Lett. **B247** (1990) 88;
B. Grinstein and M.B. Wise, Phys. Lett. **B265** (1991) 326.

[21] W.J. Marciano and J.L. Rosner, Phys. Rev. Lett. **65** (1990) 2963; (E) Phys. Rev. Lett. **68** (1992) 898;
D.C. Kennedy and P. Langacker, Phys. Rev. Lett. **65** (1990) 2967; Phys. Rev. **D44** (1991) 1591.

[22] G. Altarelli and R. Barbieri, Phys. Lett. **B253** (1991) 161;
G. Altarelli, R. Barbieri and S. Jadach, Nucl. Phys. **B369** (1992) 3;
G. Altarelli, R. Barbieri and F. Caravaglios, Nucl. Phys. **B405** (1993) 3; Phys. Lett. **B349** (1995) 145.

[23] K. Hagiwara, D. Haidt, C.S. Kim and S. Matsumoto, Z. Phys. **C64** (1994) 559; **C68** (1995) 352 (E);
K. Hagiwara, D. Haidt and S. Matsumoto, Eur. Phys. J. **C2** (1998) 95.

[24] Y. Umeda, G.C. Cho and K. Hagiwara, Phys. Rev. **D58** (1998) 115008;
G.C. Cho, K. Hagiwara and Y. Umeda, Nucl. Phys. **B531** (1998) 65; **B555** (1999) 651 (E).

[25] K. Hagiwara, Ann. Rev. Nucl. Part. Sci. **48** (1998) 463.

[26] M. Drees and K. Hagiwara, Phys. Rev. **D42** (1990) 1709;
M. Drees, K. Hagiwara and A. Yamada, Phys. Rev. **D45** (1992) 1725.

[27] G.C. Cho, K. Hagiwara and C. Kao, in preparation.

[28] G.C. Cho and K. Hagiwara, in preparation.

[29] 1998 Review of Particle Physics, C. Casao *et al.* , Eur. Phys. J. **C3** (1998) 1

[30] S. Eidelman and F. Jegerlehner, Z. Phys. **C67** (1995) 585.

[31] M. Davier and A. Hoycker, hep-ph/9801361.

[32] I. Riu, talk given at the XXXIVth Rencontres de Moriond, March 13-20, 1999.

[33] M. Veltman, Nucl. Phys. **B123** (1977) 89;
M.B. Einhorn, D.R.T. Jones and M. Veltman, Nucl. Phys. **B191** (1981) 146.

[34] M.L. Swartz, Phys. Rev. **D53** (1995) 5268.

[35] M. Felcini, talk given at the XXXIVth Rencontres de Moriond, March 13-20, 1999.

[36] T.Stelzer *et al.* , in preparation.

[37] R. McPherson, talk given at the XXXIVth Rencontres de Moriond, March 13-20, 1999.

[38] D0 Collaboration, Phys. Rev. Lett. **75** (1995) 618;
CDF Collaboration, Phys. Rev. Lett. **76** (1996) 2006;
CDF Collaboration, Phys. Rev. **D56** (1997) 1357.

[39] R. Barbieri, M. Frigeni and F. Caravaglios, Phys. Lett. **B279** (1992) 169.

[40] J. Hisano, S. Kiyoura and H. Murayama, Phys. Lett. **B399** (1997) 156.

[41] The LEP Electroweak Working Group, CERN-PPE/95-172 (1995).

[42] J.M. Cornwall and J. Papavassiliou, Phys. Rev. **D40** (1989) 3474;
G. Degrassi and A. Sirlin, Nucl. Phys. **B383** (1992) 73; Phys. Rev. **D46** (1992) 3104;
G. Degrassi, B. Kniehl and A. Sirlin, Phys. Rev. **D48** (1993) R3963. J. Papavassiliou and K. Phillippides, Phys. Rev. **D48** (1993) 4225; **D**51 (1995) 6364;
J. Papavassiliou, Phys. Rev. **D50** (1994) 5998.

[43] K. Hagiwara, S. Matsumoto and Y. Yamada, Phys. Rev. Lett. **75** (1995) 3605.

[44] A. Djouadi, P. Gambino, S. Heinemeyer, W.Hollik, C. Junger and G. Weiglein, Phys. Rev. Lett. **78** (1997) 3626;
A. Djouadi, P. Gambino, S. Heinemeyer, W. Hollik, C. Junger, G. Weiglein, Phys. Rev. **D57** (1998) 4179.